



Deliverable

Deliverable 6.4: A User-Centric Dynamic Risk Framework for Switzerland

Deliverable information	
Work package	WP6
Lead	SED/ETH
Authors	<ol style="list-style-type: none"> 1. Böse Maren, SED/ETH 2. Wiemer Stefan, SED/ETH 3. Bergamo Paolo, SED/ETH 4. Blagojevic Nikola, IBK/ETH 5. Bodenmann Lukas, IBK/ETH 6. Cauzzi Carlo Virgilio, SED/ETH 7. Chatzi Eleni, IBK/ETH 8. Clinton John, SED/ETH 9. Dallo Irina, SED/ETH 10. Danciu Laurentiu, SED/ETH 11. Diehl Tobias Christian, SED/ETH 12. Fäh Donat, SED/ETH 13. Glueer Franziska, SED/ETH 14. Han Marta, SED/ETH 15. Haslinger Florian, SED/ETH 16. Heiniger Lukas, SED/ETH 17. Janusz Paulina, SED/ETH 18. Jozinovic Dario, SED/ETH 19. Kästli Philipp, SED/ETH 20. Lanza Federica, SED/ETH 21. Lee Timothy, SED/ETH 22. Martakis, Panagiotis, IBK/ETH 23. Marti Michèle, SED/ETH 24. Massin Frederick, SED/ETH 25. Meier Men-Andrin, SED/ETH 26. Mena Cabrera Banu, SED/ETH 27. Mesimeri Maria, SED/ETH 28. Mizrahi Leila, SED/ETH 29. Obermann Anne Christine, SED/ETH 30. Papadopoulos Athanasios, SED/ETH 31. Reuland Yves, IBK/ETH 32. Roth Philippe, SED/ETH 33. Sanchez Sanchez-Pastor Maria del Pilar, SED/ETH 34. Scarabello Luca, SED/ETH 35. Schmid Nicolas, SED/ETH 36. Shynkarenko Anastasia, SED/ETH 37. Stojadinovic Bozidar, IBK/ETH 38. Valenzuela Nadja, SED/ETH
Reviewers	Helen Crowley, Eucentre Stefan Wiemer, SED/ETH
Approval	[Management Board]

Status	final
Dissemination level	Public
Will the data supporting this document be made open access? (Y/N)	[Yes]
If No Open Access, provide reasons	
Delivery deadline	2023/02/28
Submission date	2023/02/28
Intranet path	[DOCUMENTS/DELIVERABLES/File Name]

1. Introduction

- [1.1. National Seismic Hazard Model of Switzerland \(SUIhaz2015\)](#)
- [1.2. Secondary Hazards](#)
- [1.3. National Earthquake Risk Model of Switzerland \(ERM-CH23\)](#)

2. Seismic Network Operations/Observational Capabilities

- [2.1. Swiss Seismic Network](#)
- [2.2. Routine Processing](#)
- [2.3. Enhanced Velocity Models](#)
- [2.4. Enhanced Magnitudes](#)
- [2.5. Enhanced Focal Mechanisms/Moment Tensors](#)
- [2.6. Operational Double Difference Relocation](#)
- [2.7. Operational Template Matching](#)
- [2.8. ML Applications \(WP2\)](#)
- [2.9. Site Response Analyses](#)
- [2.10. Noise Interferometry](#)
- [2.11. Development of Integrated Seismic Real-time Stations \(WP2\)](#)

3. Products & Services

- [3.1. Operational Earthquake \(Loss\) Forecasting \(OEF & OELF\) \(WP3, WP4\)](#)
- [3.2. Earthquake Early Warning \(EEW\) \(WP4, WP5\)](#)
- [3.3. ShakeMaps](#)
- [3.4. Rapid Impact Assessment \(RIA\) \(WP4\)](#)
- [3.5. Structural Health Monitoring \(SHM\) \(WP3\)](#)
- [3.6. Recovery and Rebuilding Efforts \(RRE\) \(WP4\)](#)

4. Operation & Communication

- [4.1. Operation, IT \(WP8\)](#)
- [4.2. Communication & Societal Perspective \(WP5, WP8\)](#)

5. Conclusions & Outlook

6. References

1. Introduction

M. Böse, S. Wiemer

Europe is exposed to a high level of earthquake risk due to its tectonic situation, high population density, business value, and the age and condition of buildings. Even in areas of moderate seismic activity, such as Switzerland, earthquakes have the potential for significant loss, as they are low-probability but high-consequence events with potential costs exceeding Euro 100 billion. The 2015 Swiss Federal Office for Civil Protection risk report ranked earthquakes as the third highest risk for Switzerland, behind electricity shortages and pandemics (FOCP, 2020). Building codes and retrofitting are the primary and most effective measures to reduce earthquake risk, but emerging technologies, such as Earthquake Early Warning, also offer opportunities to improve resilience and reduce potential loss.

Here we report the progress made in creating a user-centered dynamic risk framework (**Figure 1**) in Switzerland that considers earthquake hazard and risk as integrated and dynamically evolving over time, both on short-term (e.g., due to a nearby active seismic sequence or changing day/night time building occupancy) and long-term scales (e.g., due to rapid urbanization and building changes). This includes the development of various services, products, and research at the Swiss Seismological Service (SED) and the Institute of Structural Engineering (IBK) at ETH Zurich over the past couple of years, supported through the European Horizon-2020 project *Real-time earthquake rIsk reduction for a ReSilient Europe* (RISE), but building synergistically on other projects. RISE takes an integrative and holistic view of risk reduction, proposes a framework that uses all available information to assess risk at various stages of the earthquake cycle, and encourages widespread dissemination and communication of the information.

Over the last decade, the SED has made significant advancements in the seismic observational capabilities in Switzerland, thanks to the implementation of denser sensor arrays and advanced data-processing. The SED operates the high-quality, low-latency Swiss Seismic Network consisting of short-period, broad-band, and strong-motion sensors. As described in this deliverable, recent improvements in velocity models, magnitude calibrations, focal mechanism and moment tensor computations, as well as recently implemented operational double difference relocation, template matching, and machine-learning techniques have led to an even more complete and detailed understanding of seismicity throughout Switzerland. Improved site response characterizations, noise interferometry to advance earthquake predictability research, and the development and testing of new sensors have also contributed to this progress. While the basics of template matching, machine learning, and relative relocation have been available for a while, most of the remaining challenges and complexities concerned pre- and post-processing of data, quality control, data management, and other factors that previously

required substantial manual intervention and limited real-time routine applications. The SED addressed these challenges in Switzerland by focusing on operationalizing advanced processing for denser and more diverse real-time seismic networks.

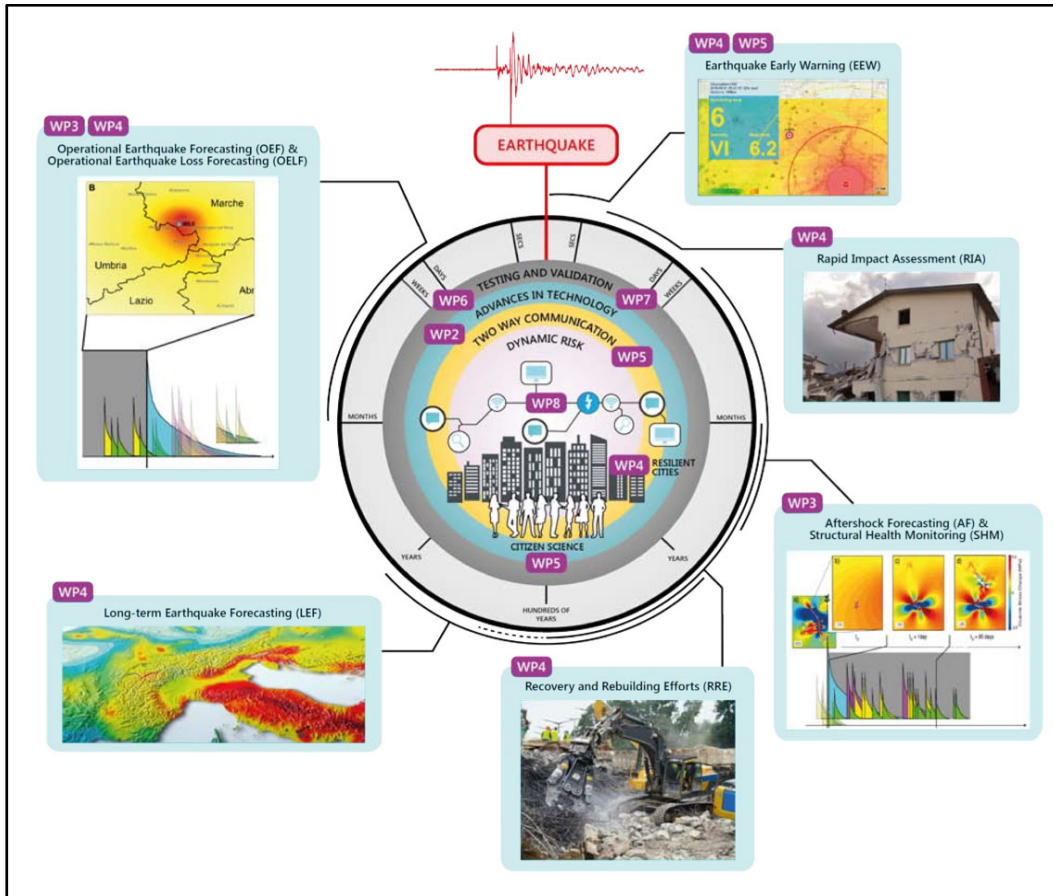


Figure 1. Schematic representation of the dynamic risk concept promoted in RISE, with relevant work packages (WPs) marked (copied from RISE proposal).

The advancements in observational capabilities are crucial for improving tools for Operational Earthquake (Loss) Forecasting (OEF and OELF), Earthquake Early Warning (EEW), and Rapid Impact Assessment (RIA)¹. Current first-generation OEF tools in Switzerland are able to identify periods and regions of increased seismic risk in the short-term. However, more advanced and thoroughly tested forecasting algorithms, informed by improvements in observational capabilities and forecast models, have the potential to greatly reduce uncertainties and improve forecasting accuracy. Similarly, EEW systems use distributed sensors and rapid algorithms to provide preliminary event information and alert people in real-time, allowing for actions to be taken before the shaking occurs. RIA systems can quickly assess the damage and likelihood of another event, enabling rapid response and informed decision-

¹ RIA is conceptually equivalent to what is referred to as RLA (Rapid Loss Assessment) in other RISE deliverables. For CH, however, it was decided that the word 'impact' would be clearer to the public.

making for rescue and rebuilding efforts. Structural health monitoring (SHM) offers the tools to analyze continuous sensor data and retrieve information regarding the structural state (health) of a structure. Finally, by reducing the downtime of buildings and infrastructure systems, rapid recovery reduces negative social and economic impacts.

This report is divided into four chapters: Chapter 1 provides an overview of the earthquake hazard and seismic risk in Switzerland. Chapter 2 describes the seismic network operations of the SED (RISE WP2 and other projects). Chapter 3 presents risk-related products and services at the SED/IBK (RISE WP3, WP4, WP5). Finally, Chapter 4 provides an overview of the operation of these services, as well as the communication with the public and stakeholders (RISE WP5, WP8).

1.1. National Seismic Hazard Model of Switzerland (SUIhaz2015)

M. Böse, J. Clinton

According to the Swiss Seismic Hazard model (SUIhaz2015; Wiemer *et al.*, 2016), Switzerland has a high likelihood of experiencing earthquakes (**Figure 1.1.1**). Ground shaking is the hazard assessed by this model. On average, an earthquake with a magnitude of 5 can be expected to occur every 8 to 15 years, despite the last earthquake of this magnitude happening roughly 25 years ago (Vaz GR, 1991). Buildings can suffer significant damage, depending on the location and depth of such an earthquake. Earthquakes with a magnitude of 6 or greater, which can cause widespread and severe damage, occur every 50 to 150 years on average and can happen at any time and any place in Switzerland. The last earthquake of this magnitude happened in Upper Valais in 1946 (Sierre VS, 1946). Valais is the region with the greatest risk of earthquakes, followed by Basel, Grisons, the St. Gallen Rhine Valley, Central Switzerland, and other parts of the country.

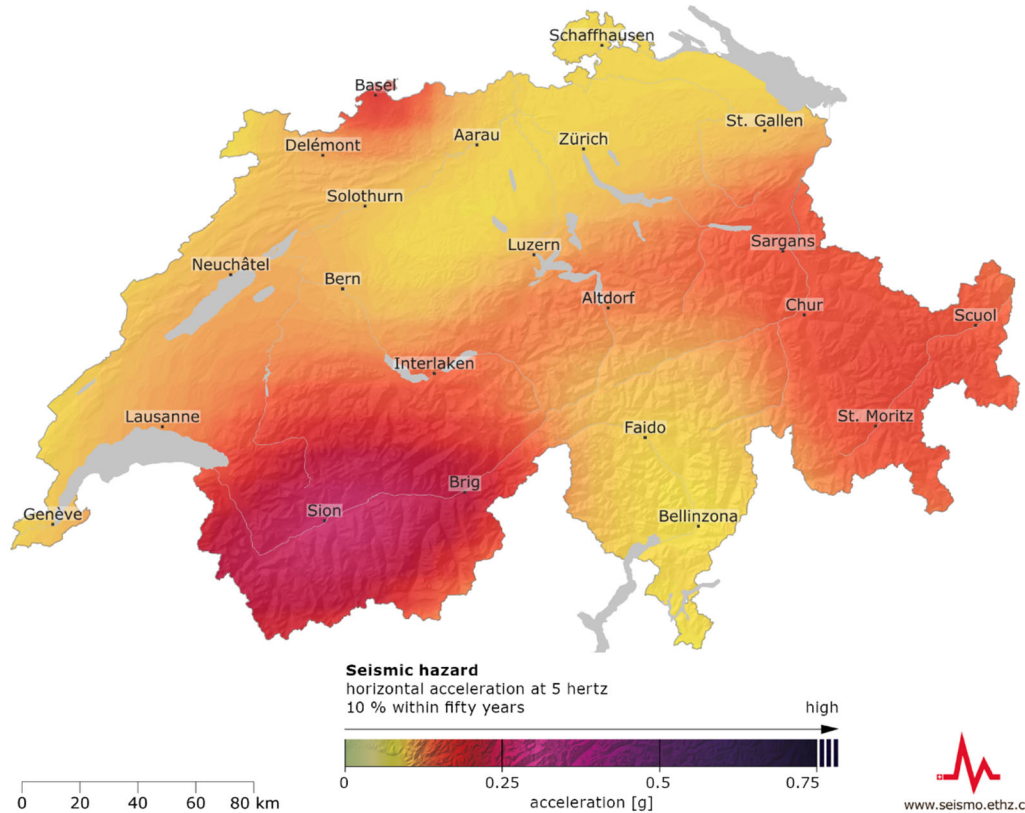


Figure 1.1.1. Swiss Hazard Map (SUIhaz2015) showing the horizontal acceleration at 5 Hz; the probability of a building constructed on rocky subsoil experiencing this is 10 % within fifty years (500 years). On average, 5 Hz represents the natural frequency of buildings with two to five floors, which make up the largest proportion of constructions in Switzerland. 500 years is the value that underlies the Swiss seismic building codes: an earthquake-resistant residential or office building should be able to withstand an earthquake that occurs where the building is situated within 500 years on average.

On average, between 1000 and 1500 events are manually located in and around Switzerland every year. **Figure 1.1.1** shows all events located in Switzerland since 2009. The catalog may be accessed using the standard FDSN event web service². The majority of the catalog consists of earthquakes, though there are significant numbers of quarry blasts included. Also more rare events such as landslides, sonic boom, and plane crashes are included.

² <https://eida.ethz.ch/fdsnws/event/1/query?>



Figure 1.1.2. Map of Switzerland and surrounding area showing all seismicity included in the SED catalog since 2009. Dot size scales with magnitude.

1.2. Secondary Hazards

P. Bergamo, D. Fäh, A. Shynkarenko, P. Janusz, F. Glueer

The damaging effect of earthquakes is not exclusively related to strong ground motion. In specific geographic settings, secondary hazards (e.g., lake tsunamis, landslides, and liquefaction) may be also triggered by earthquake ground motion. A number of studies in historical and paleo-seismology (Fritsche *et al.*, 2012; Fäh *et al.*, 2012; Kremer *et al.*, 2020) have demonstrated the particular relevance of earthquake-induced phenomena for Switzerland. Its territory is prone to such phenomena due to large and deep peri-alpine lakes, steep and potentially unstable slopes, and alluvial basins with surficial water table. These settings are susceptible, respectively, to lake tsunamis and impulse waves, landslides/rockfalls, and liquefaction. Besides the effort in historical and paleo-seismology, research at SED has therefore focused on studies aiming at estimating in a quantitative fashion the hazard and risk related to such earthquake-induced phenomena.

Rockfalls and landslides. Rockfalls and landslides, either spontaneous or earthquake-triggered, are relevant hazards for the rugged Swiss territory (e.g., landslide at Piz Cengalo³). The SED has devoted significant effort to the study of such phenomena. The acquisition, processing, and interpretation techniques proper of ambient-vibration-based geophysical imaging have been successfully adapted to

³ e.g. https://en.wikipedia.org/wiki/Piz_Cengalo

the characterization and long-term monitoring of unstable slopes (e.g., Burjanek *et al.*, 2018; Kleinbrod *et al.*, 2018; Häusler *et al.*, 2021, 2022). Furthermore, the installation of a network of temporary seismic stations at the sites of instabilities (**Figure 1.2a**) has allowed to model their local seismic response and relate it to their internal structure (Kleinbrod *et al.*, 2017a,b; Weber *et al.*, 2021). Site response variability due to environmental conditions and changes in the characteristics of the instability were detected and interpreted (Häusler *et al.*, 2021, 2022). Geophysical surveys and earthquake monitoring are also accompanied by numerical modeling studies (Burjánek *et al.*, 2019; Glueer *et al.*, 2021), which enables predicting the behavior of unstable rock masses subject to seismic loading. The body of knowledge thus collected in the field of earthquake-induced mass movements has also flown into the SED ShakeMaps application for the prediction of rockfalls/landslides likelihood after significant events (see section 3.3).

Lake tsunamis. Destructive tsunamis are known to have occurred in Swiss lakes in the past (Fritsche *et al.*, 2012; Hilbe & Anselmetti, 2014; Kremer *et al.*, 2012, 2017, 2022). For a significant portion, a link with specific earthquakes can be established, triggering the collapse of subaerial and/or submerged lake slopes, and hence induce impulse waves and lake tsunamis. To characterize submerged lake sediments that failed in the past or are likely to fail and trigger a tsunami in the future, the knowledge acquired at SED for onshore geophysical surveys (see section 2.9) has been translated to the offshore environment (submerged lake slopes). Ambient vibration techniques were successfully applied – jointly with in-situ and laboratory geotechnical surveys – to determine the geomechanical properties of lacustrine sediments in Lake Lucerne (Shynkarenko *et al.*, 2021, 2022; Lontsi *et al.*, 2022; see **Figure 1.2b**). The earthquake response of such sediments was also directly measured using seismic stations (Ocean Bottom Seismometers) deployed on the lake floor (Shynkarenko *et al.*, 2023), again by applying methods and procedures developed for onshore site amplification studies (see section 2.10). Such detailed geophysical and geotechnical data is required to refine – from a physics-based point of view – numerical models used for hazard and risk studies related to lake tsunamis in Switzerland (Strupler *et al.*, 2018, 2020).

Liquefaction. Extended sandy and silty surficial sediments with a shallow water table, both prerequisites for the onset of liquefaction phenomena, characterize the alluvial basins of Switzerland (e.g., valley beds). However, given the significant return period for earthquakes able to trigger liquefaction, this phenomenon is sparsely documented (Fritsche & Fäh, 2009; Fritsche *et al.*, 2012). Nevertheless, due to the recent urbanization in alpine valleys over areas with soil with poor bearing capacity, liquefaction may be more relevant nowadays than in the past (from the risk point of view). In the absence of vast empirical data, at SED the focus has shifted to the identification of areas and formations which may be prone to liquefy and to the estimation of the required ground motion level. Refined tools for the interpretation of the Cone Penetration Test (CPT, a geotechnical test standardly employed to assess the soil susceptibility to liquefaction) have been developed to estimate the friction and dilation properties of soil (Roten, 2014; Roten *et al.*, 2014), which are then fed to fully nonlinear simulations (Bonilla *et al.*, 2005). This allows predicting which layers liquefy and at which level of ground

motion (Roten *et al.*, 2009; Janusz *et al.*, 2022a, 2022b). Over the years several sites – with suitable geology - have been surveyed with CPT, jointly with geophysical measurements (Hobiger *et al.*, 2021), to assess their liquefaction potential. Some sites have been equipped with permanent downhole strong motion and pore pressure sensors. Presently, a study focusing on the area of Lucerne is underway (Janusz *et al.*, 2022b, 2022c), showing the potential of liquefaction in the densely populated city center for a broad range of ground motion levels, as well all strong non-linear behavior of the modeled soil (e.g. **Figure 1.2c**).

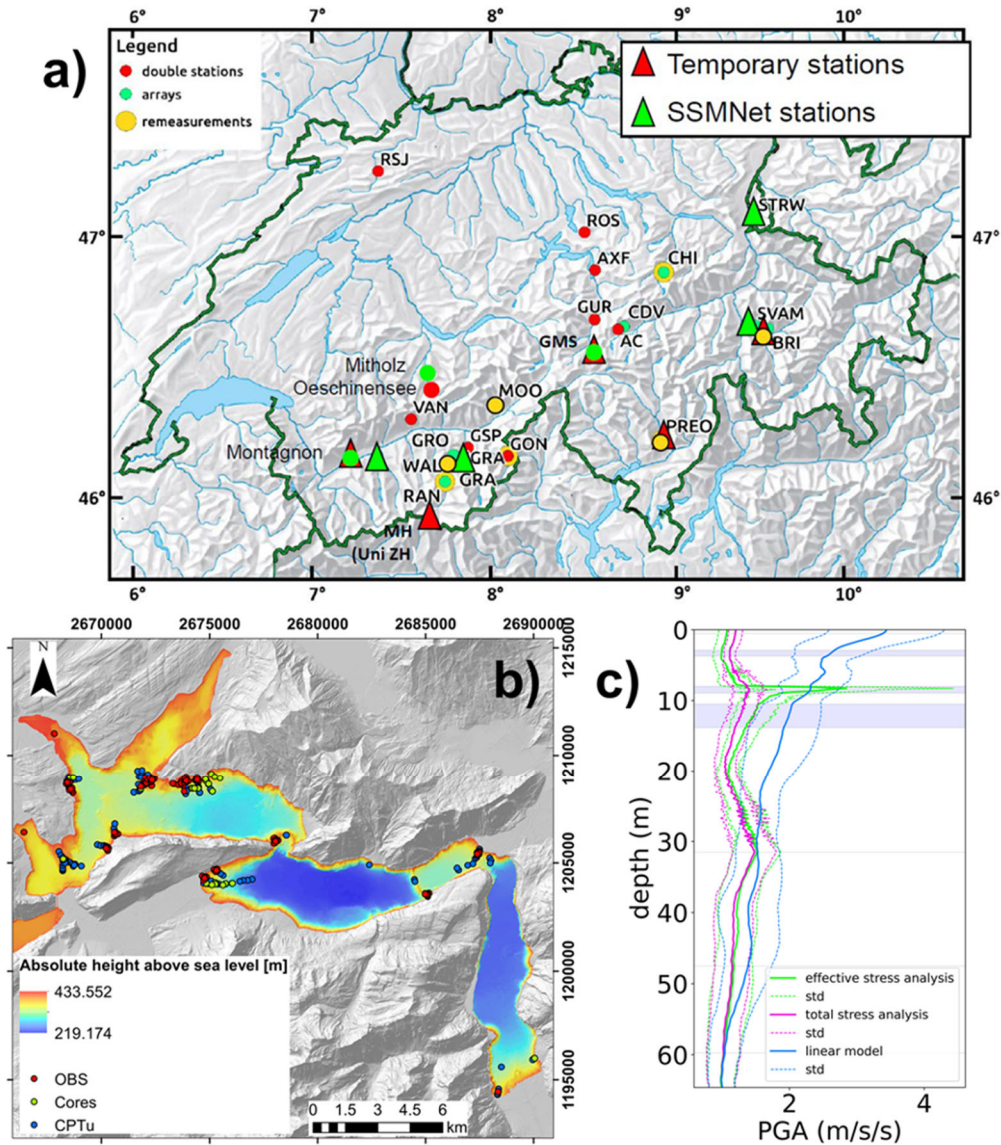


Figure 1.2. a) Installed seismic stations (triangles) and geophysical measurements (circles) targeting rock instabilities and potential landslide areas. b) Installed ocean bottom seismometers (OBS), geophysical and geotechnical measurements targeting the submerged slopes of Lake Lucerne (figure from Shynkarenko, 2023). c) Example of nonlinear soil response simulation at the site of seismic station SLUW (Lucerne); liquefaction occurs in a sandy layer at ~ 8.5 m depth (figure from Janusz *et al.*, 2022c).

1.3. National Earthquake Risk Model of Switzerland (ERM-CH23)

A. Papadopoulos, L. Danciu, P. Roth

Earthquake hazard and risk models provide the basis for long-term mitigation actions to reduce the consequences of earthquakes and strengthen societies' resilience to disasters. While seismic hazard has been thoroughly studied in Switzerland over the years (Giardini *et al.*, 2004; Wiemer *et al.*, 2016), no previous formal attempt to quantify seismic risk was available until recently in the public domain. To fill this gap, the SED was commissioned by the Federal Council, to devise the first National Earthquake Risk Model of Switzerland (ERM-CH23), in cooperation with the Federal Office for the Environment (FOEN) and the Federal Office for Civil Protection (FOCP). After a period of development, the official release of the model in March 2023 marked a major milestone.

The ERM-CH23 is implemented for use with the open-source OpenQuake engine (Pagani *et al.*, 2014), developed by the Global Earthquake Model (GEM) foundation. As most contemporary risk models, ERM-CH23 follows a modular structure (Mitchell-Wallace *et al.*, 2017), with three generally decoupled components pertaining to seismic hazard, structural vulnerability, and exposure. These components were developed through collaboration with national and international partners. Unlike past attempts that sought to assess earthquake risk at a continental (Crowley *et al.*, 2021) or global scale (Silva *et al.*, 2020), ERM-CH23 is largely supported by high-quality local data. Of note is the database of more than 2 million building objects that was compiled by the FOEN. Together with ground surveys to assess the frequency of different building material, conducted by partners at the École Polytechnique Fédérale de Lausanne (EPFL), they underpin the ERM-CH23 exposure model. The value of such a database is further accentuated when paired with a high-resolution site amplification subcomponent. A culmination of many years of efforts and expertise within the SED, a national site amplification model was built as part of ERM-CH23, using statistical techniques constrained on local site response measurements at instrumented sites (Bergamo *et al.*, 2022).

The risk analysis follows a typical event-based approach. It starts with the generation of stochastic earthquake catalogs, followed by the simulation of random ground motion fields for each generated rupture, and the computation of associated losses. To capture the wide range of uncertainty present in such models, a logic tree with several branch levels was defined. The first branching level refers to the intensity measure used to describe the ground shaking; two alternative pathways are followed, the primary one using spectral acceleration, and the secondary one using macro-seismic intensity. Further branching levels were defined for ground motion prediction, site amplification, and exposure.

ERM-CH23 assesses a few different loss types, namely structural/nonstructural economic loss, contents economic loss, fatalities, injuries, and people in need of shelter. Standard risk metrics such as average annual loss (AAL) or losses associated with specific return periods are readily provided. **Figure 1.3**

illustrates the spatial pattern of risk across Switzerland via a composite risk index combining average annual structural/nonstructural loss and fatalities. Naturally, the highest risk is seen in urban areas with high density of exposure (buildings and population). Regions exposed to higher seismicity (cantons Basel or Valais), and/or featuring areas where high site amplification is expected (such as parts of the canton of Valais), stand out even more in the map.

In the years to come, ERM-CH23 is expected to raise public awareness for earthquake risk, enable cantonal and national authorities to form updated views of their risk, and support them in drawing up mitigation actions. It should also serve as a valuable resource for the insurance and reinsurance industry, and as a point of reference within the scientific community. Lastly, the ERM-CH23 serves as the basis for additional tools and systems being developed by the SED, such as RIA and OELF. Such systems are based on the primary subcomponents of the ERM-CH23 to provide near-real-time results and vital information in the immediate aftermath of earthquakes.

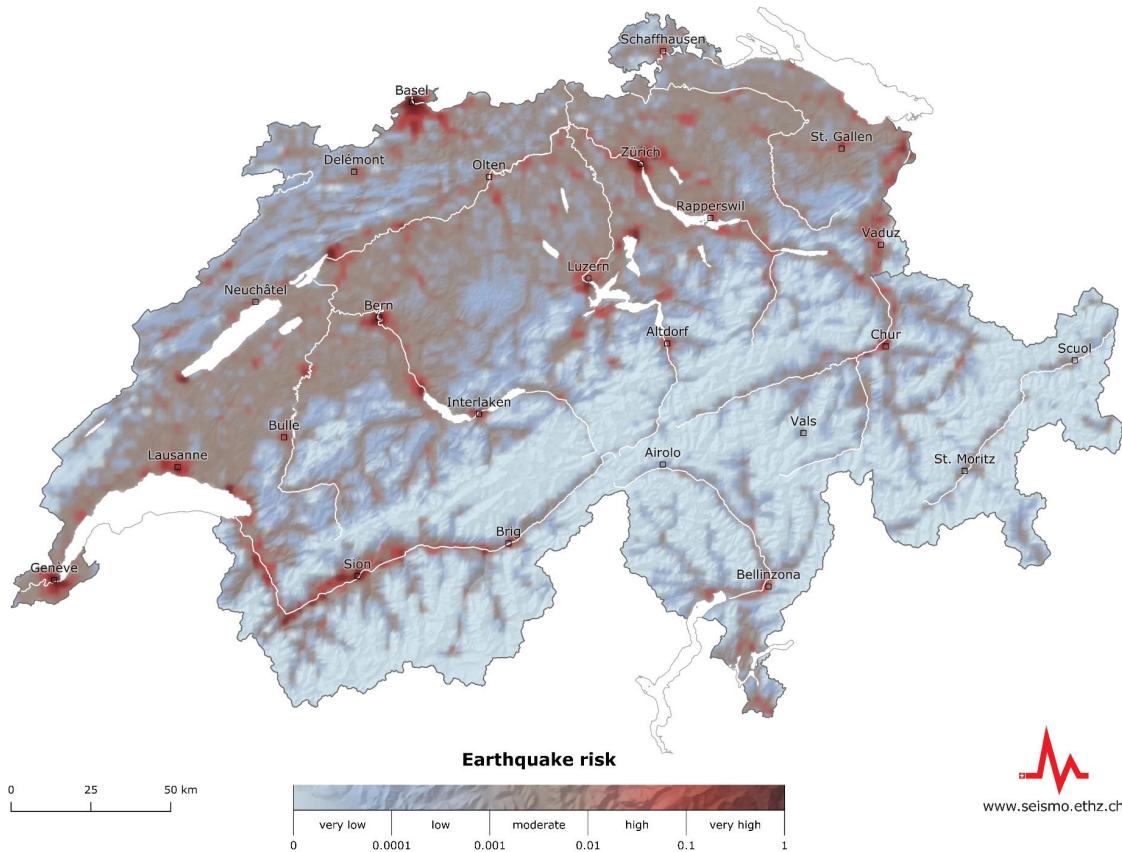


Figure 1.3. The earthquake risk map of Switzerland. The color scale refers to a composite index based on average annual structural/nonstructural loss and fatalities.

2. Seismic Network Operations/Observational Capabilities

2.1. Swiss Seismic Network

J. Clinton, F. Massin

The Swiss Seismic Network (**Figure 2.1.1**) consists of about 220 permanent stations (CH network code; SED, 1983). The goal of this network is to monitor seismicity of the territory, support science, and assess the seismic risk. The network consists of two main classes of stations. The backbone broadband set of stations (known as the 'SDSNet') comprising about 50 stations, include very broadband seismic sensors at quiet locations with vault conditions and are evenly distributed across the country. These stations ensure the network can detect and accurately locate microseismicity occurring anywhere across Switzerland. Each site also includes a strong motion accelerometer. About 150 stations make up the strong motion network (known as 'SSMNet') that chiefly targets monitoring the areas of the country with the high hazard and risk, hence sites are mainly in the urban areas across the country and focus on regions of highest risk, such as Basel and the Rhone valley in the Valais. Other stations with targeted purpose, such as geothermal monitoring, comprise the rest of the network, and typically include only broadband or short period sensors. The broadband sensors are predominantly Streckeisen STS2 and STS2.5 and Nanometrics T240. Strong motion sensors are predominantly Kinematics EpiSensor. All stations operate modern ultra-low latency digitisers (majority are Nanometrics Centaur, though there are significant numbers of Nanometrics Taurus and Kinematics Q330) – the network hardware is optimized for EEW. The majority of sensors are acquired at sampling rates between 200-250 sps.

The network also monitors about 70 temporary stations deployed in Switzerland under various different network codes that have different targets. Projects include aftershock stations and seismic sequences (network code 8D); stations targeting monitoring of mass movements and landslides (9S); glacier monitoring (4D); risk studies (XY); Bedretto underground laboratory (8R). To augment the ability to detect and characterize seismic events, an additional ~10 stations operated by external providers are also included in the SED processing. This includes a small network in CERN (C4); collections of stations focused on monitoring sites of geothermal exploration (5A); and a Matterhorn Observatory (1I). Finally, for regional monitoring, about 50 stations operated by seismic agencies in neighboring countries are also included in real time. **Figure 2.1.1** shows all stations currently monitored by the Swiss Seismic Network. The SED also operates other temporary stations for various projects located outside of Swiss borders, for example a nodal network was operated in Iceland in 2021 (YM).

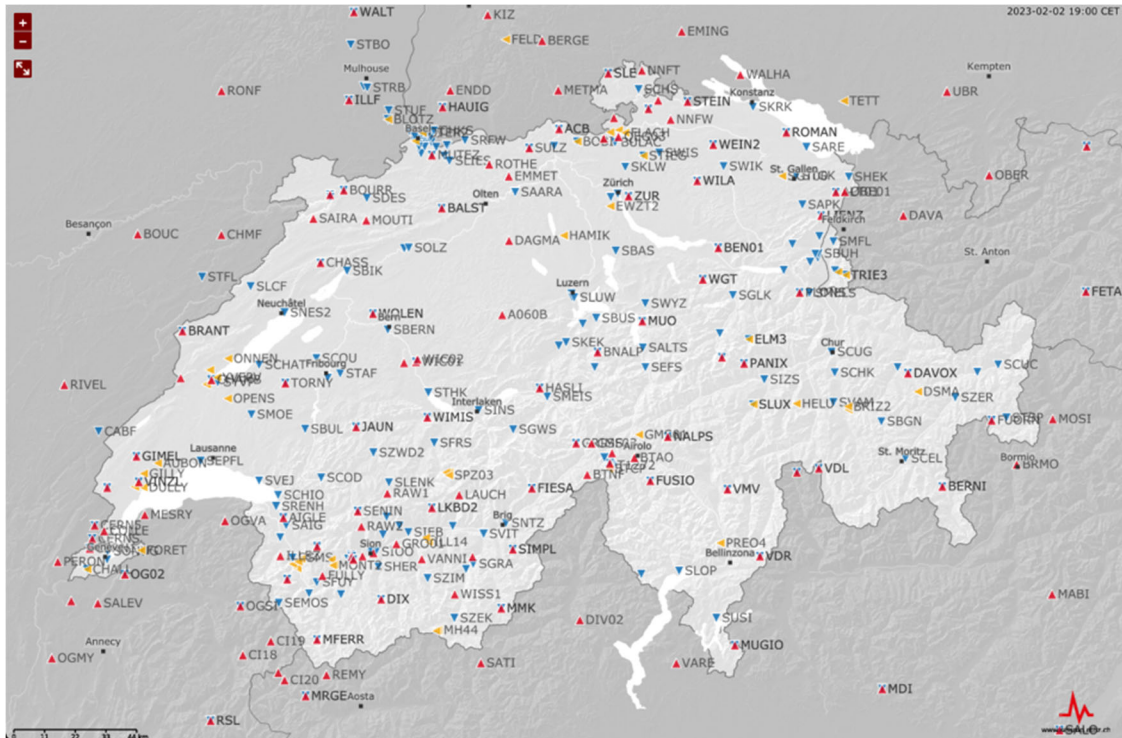


Figure 2.1.1. Map of Switzerland and surrounding area showing all seismic sensors monitored by the Swiss Seismic Network in January 2023. Red triangles: broadband sensors; yellow triangles: short period sensors; blue triangles: strong motion sensors. Stations include permanent and temporary stations operated by the SED, as well as stations operated by external partners in Switzerland and neighboring countries.

The last 20 years have seen a sustained growth in the number of stations. **Figure 2.1.2** presents the change in station numbers over time for the Swiss national network. Continuous data from broadband sensors began to be regularly archived from 1999. The growth in the SED archive is also shown in **Figure 2.1.2**. Today, about 20GB of data is collected every day, and the total archive reaches nearly 100TB. The SED Seismic Network operates an EIDA node (Strollo *et al.*, 2021). The majority of the waveform data is open and can be accessed using community standard FDSN web services for discovery⁴ and waveform download⁵.

⁴ <https://eida.ethz.ch/fdsnws/station/1/query?>

⁵ <https://eida.ethz.ch/fdsnws/station/1/dataselect?>

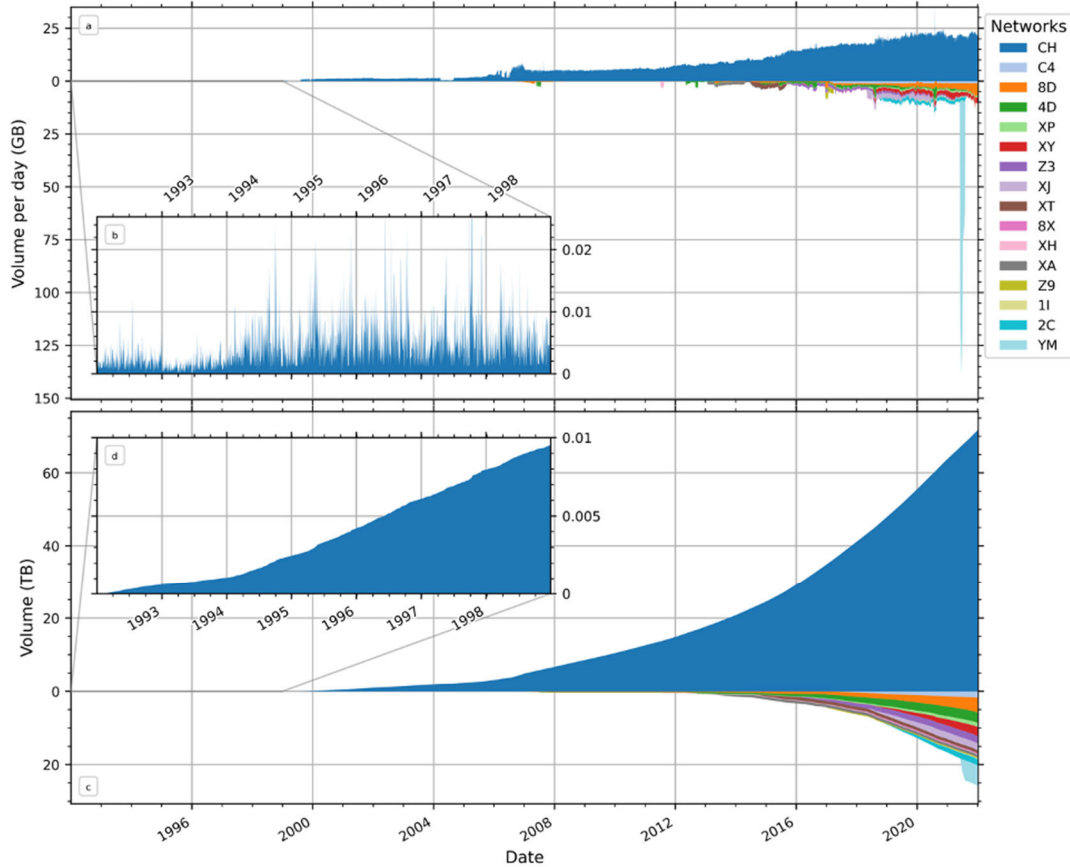
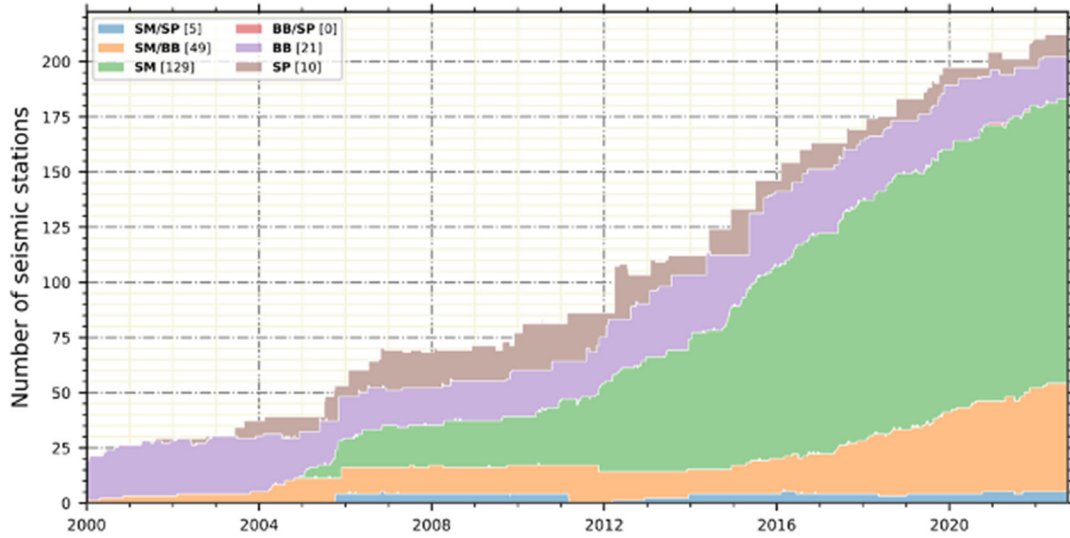


Figure 2.1.2. Top: growth in number of sensors in the Swiss Seismic Network between 2000 to 2023, color indicates sensor type. Middle: volume of data recorded in the SED waveform data archive each day, from 1992-2021, color indicates network code. Permanent network codes are above 0, temporary network codes are below 0. Note explosion of data in mid-2021 resulting from nodal experiment with network code YM. Bottom: as middle, except showing cumulative size of archive, for each network code. Today, the archive is nearly 100TB in volume.

2.2. Routine Processing

J. Clinton, F. Massin

Since 2012, the Swiss Seismic Network has been using SeisComP (Helmholtz Centre Potsdam GFZ German Research Centre for Geosciences and GemPa GmbH, 2008) for earthquake monitoring and seismic data processing. SeisComP supports real-time data acquisition, data archival and re-distribution, automatic earthquake detection and quantification, and manual earthquake review and catalog management. Beyond the standard modules for automatic locations (*scautopick*, *scautoloc*, *nonlinloc*, *scamp*, *scmag*, *scevent*), specific modules have been developed either internally or with support from GemPa, and introduced for advanced processing. These include:

1. *scwfparam* for providing engineering parameters and specifically input to ShakeMaps (see section 3.3);
2. a suite of modules (*scenvelope*, *scvsmag*, *scfinder*) for EEW (see section 3.2)
3. *scrtdd*, a module that delivers real time double difference earthquake locations (see section 2.6); and
4. *scdetect*, a module that creates events detected by template matching approaches (see section 2.7).

Each of these modules and the resulting products are described in further detail later in the document. A further enhancement to SeisComP specific to the SED is the integration of MIhc, a Swiss-specific local magnitude scale that uses an attenuation model valid from about 2 km distance out to 500 km, and from magnitudes spanning MI1.0-5.0, as well as integrating site-specific amplification values (see section 2.10).

The current features of basic real-time automated processing are:

- event triggering uses station-specific STA/LTA thresholds that take into account the background noise of the station. The best stations (generally broadband sensors in the Alps) use a ratio of 3; the worst stations (such as strong motion sensors in urban environments near trains, trams, or vehicular traffic) use a ratio of 100;
- refined post-picking using Bear and AIC pickers improve the precision of picks. AIC S-picks are also created;
- picks are associated using *scautoloc* or *scanloc*; events are located using 1D velocity model to provide origins;
- origins with refined locations are provided using a 3D velocity model and *nonlinloc* (see section 2.3);
- origins continue to be updated as new picks arrive during an on-going event;

- magnitudes are provided for all origins;
- origins are combined and the best origin is selected using a SED developed origin score that takes into account the number of picks, pick residuals, and azimuthal gap;
- When earthquakes are larger than M2.5, alerts are sent out to multiple stakeholders (see section 4.2), a ShakeMap is created (see section 3.3), and the strong motion portal⁶, providing access to event-based waveform and parametric data, is populated.
- Manual review is performed using the SeisComP *scolv* gui. For large events with M>3.0, manual moment tensor results are calculated using the SeisComP *scmtv* gui (see section 2.5).
- An additional magnitude based on spectral peaks, *Mwspec*, is also calculated for manually reviewed solutions using in-house software (see section 2.4).
- The earthquake catalog is curated through *scolv*.

2.3. Enhanced Velocity Models

T. Diehl, T. Lee, F. Lanza

High-resolution seismotectonic interpretation of natural and induced seismicity in Switzerland nowadays requires absolute hypocenter accuracy at scales of one kilometer and less in order to associate earthquakes with geologically or geophysically mapped faults. This was demonstrated, for instance, for the induced seismicity related to the geothermal project in St. Gallen in 2013 (Diehl *et al.*, 2017). Achieving such sub-kilometer hypocenter accuracy requires improved 1D or 3D P- and S-wave velocity models at different scales. In addition, accurate velocity models provide information on the source-sided seismic velocity structure, which can help to constrain the lithology hosting seismicity in the crust as shown by Diehl *et al.* (2017). Especially the question whether seismicity occurs in sedimentary units or in the crystalline basement is of importance for understanding present-day tectonic processes in the Alps and its foreland (e.g., thin-skinned vs. thick-skinned deformation). In turn, this knowledge is of key importance for many geotechnical applications such as geothermal exploration and site evaluation for geological waste repositories. Finally, improved 3D velocity models in combination with attenuation models are the base parameters for realistic ground-motion simulations. Over the past decades, several projects have therefore been initiated and carried out to improve the existing velocity models at different scales.

A first 3D P-wave model for Switzerland was computed by Husen *et al.* (2003) from a local earthquake tomography (LET), complemented by information from seismic refraction experiments. The horizontal node spacing of this model was 15x15 km. At that time, the S-wave data was not sufficient for a 3D S-wave model and hypocenter locations with this model were derived with a constant V_p/V_s ratio. This model has been used by the SED for bulletin locations since about 2004. In 2009, a regional 3D LET P-wave velocity model was computed, which imaged large parts of the Alpine crust with a grid-node

⁶ <http://strongmotionportal.seismo.ethz.ch/home/>

spacing of 25x25x15 km (Diehl *et al.*, 2009). This model was used by the SED for locating regional seismicity outside of Switzerland since about 2013. However, none of these P-wave models was sufficient to provide the targeted sub-kilometer accuracy. To achieve this and to benefit from the significant increase in quantity and quality of arrival-time data since about 2010, a refined Pg and Sg LET model (parametrization 10x10x4 km) was computed, including data through 2020 (Diehl *et al.*, 2021). Diehl *et al.* (2021) demonstrate that a sub-kilometer accuracy can be achieved in most parts of Switzerland by using Pg and Sg phases in combination with an accurate 3D velocity model and the dense seismic network operated by the SED. A horizontal cross-section of the model at a depth of 4 km is shown in **Figure 2.3**. The new model has been used for relocation and high-resolution seismotectonic interpretations in several studies so far (Lanza *et al.*, 2022; Lee *et al.*, 2023; Diehl *et al.*, 2023) and used as standard model for bulletin locations by the SED since June 2022.

The LET model of Diehl *et al.* (2021) was locally even further improved by Lee (2023), by applying a staggered-grid approach resulting in a 5x5x3 km model parametrization for the region of the Rhone-Simplon Fault Zone (RSF in **Figure 2.3**) in southwestern Switzerland. This model provides fine-scale images of seismic velocities related to tectonic units and partly fault zones in the transition between Central and Western Alps. In addition, the SED currently works on an extension of the Diehl *et al.* (2021) models to the entire crust, a Swiss-wide 3D Qp and Qs attenuation model as well as, in collaboration with groups at ETH and Istituto Nazionale di Geofisica e Vulcanologia (INGV), on a new Alpine-wide 3D P-wave crustal model using the data of the AlpArray experiment.

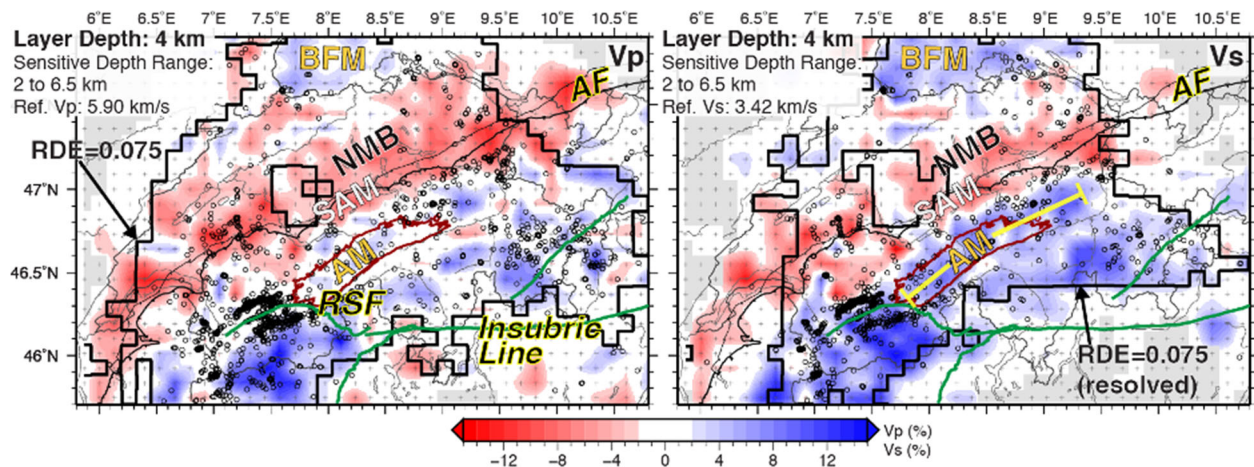


Figure 2.3. Horizontal cross-section through the 3D Vp and Vs tomographic model of Diehl *et al.* (2021) at a depth of 4 km. The velocity structure is shown as percentage change relative to the 1D initial reference models. Bold black contours include areas that are well and fairly well resolved ($RDE \geq 0.075$); areas outside these contours have poor or no resolution. Circles mark contributing earthquakes located within the corresponding depth interval. Dark red line shows the outline of the Aar Massif (AM) exposed at the surface; AF, Alpine Front; BFM, Black Forest Massif; NMB, Northern Molasse Basin; RSF, Rhone-Simplon Fault; SAM, Subalpine Molasse.

2.4. Enhanced Magnitudes

C. Cauzzi

In the last few years, the SED has updated its strategy for magnitude determination to make it fully consistent with the state-of-the-art in engineering seismology and seismic hazard studies in Switzerland, and to optimize the use of its dense seismic monitoring infrastructure. Among the changes implemented are: (a) the adoption of a new local magnitude relationship ML_{hc} ; (b) inclusion of local magnitude station corrections based on empirically observed (de)amplification with respect to the Swiss reference rock velocity model and associated predictions; (c) seamless computation of M_w based on spectral fitting (M_wSpec) of recorded Fourier Amplitude Spectra using a Swiss specific model. For more information, please check the following references: Racine *et al.*, 2020; Edwards *et al.*, 2010; Edwards *et al.*, 2015. ML_{hc} and M_wSpec (when available) were calculated and added to the SED catalog for all events back to 2009/01/01. Since November 2021, ML_{hc} has been the authoritative local magnitude used by the SED. The SED earthquake catalog is openly available using, for example, the FDSN event web service⁷. There are plans to further improve magnitude determination at SED in the coming years within the framework of a SNF-funded research project.

2.5. Enhanced Focal Mechanisms/Moment Tensors

M. Mesimeri, T. Diehl, J. Clinton

The SED operates and maintains a dense seismic network that allows for robust calculation of high-quality, first-motion focal mechanisms. For earthquakes with an adequate number of manually revised P-wave polarities, sufficient to constrain unique solutions, traditional first-motion focal mechanisms have been calculated from instrumental recordings of the SED since 1976. Additional mechanisms back to 1961 are listed in Kastrup *et al.* (2004). The methods used and the completeness of these solutions have varied over the years (for an overview see, e.g., Kastrup *et al.*, 2004; Marschall *et al.*, 2013; Diehl *et al.*, 2023). Since 2013, the software HASH (Hardebeck & Shearer, 2002) has been consistently used to invert for focal mechanisms and their uncertainties. Since 1996, focal mechanisms are published in annual and bi-annual reports of the SED (e.g., Baer *et al.*, 1997; Deichmann *et al.*, 2000; Diehl *et al.*, 2021a) and are used for seismo-tectonic interpretation along with high-resolution earthquake locations, especially during outstanding earthquake sequences in Switzerland and surrounding regions. For these reports, a solution was usually attempted for events with local magnitudes $ML \geq 2.5$. However, the focal-mechanism catalog of the SED (compiled in large parts by Nicolas Deichmann and Tobias Diehl) also includes solutions for smaller magnitudes, especially for more recent periods. On the other hand, due to the significant manual effort and the limited additional benefit, events with $ML \geq 2.5$ with

⁷ <http://www.seismo.ethz.ch/en/research-and-teaching/products-software/fdsn-web-services/>

mechanisms similar to published solutions of a sequence were sometimes not included. Therefore, it is not possible to define a homogeneous completeness of the focal-mechanism catalog of the SED. The current focal-mechanism catalog of the SED contains 414 (mostly) high-quality solutions for ML between 0.9 and 5.1. Mechanisms of earthquakes between 1961 and 1998 (138 solutions) are published in Kastrup *et al.* (2004).

For earthquakes with $M_I \geq 3.0$, the SED attempts to compute a moment tensor using algorithms that are based on full broadband waveform inversion. The moment-tensor inversion methods used at the SED have varied over time (Braunmiller *et al.*, 2005; Vakar *et al.*, 2017). Similar to the first-motion catalog, no homogeneous completeness can be defined - reliable moment tensor solutions can sometimes be retrieved for magnitudes as low as $M_I 2.9$ (especially during summer when background microseismic noise is reduced) though high-quality solutions are typically reliably obtained from $M_I \geq 3.5$. Since 2015, we use the SeisComP module *scmtv* in the routine process (Vackář *et al.*, 2017) and publish the solutions in the bi-annual reports. Methodologically, the algorithm uses pre-computed Green's Functions generated by incorporating a 1D P- and S-wave velocity model, and for the inversion a least square scheme is adopted (Dreger, 2003). We assume that the isotropic component is zero, the epicentral coordinates are fixed, with variable depth, and the source time function is fixed. This method fits well with the magnitudes and mechanisms predicted by earlier methods for legacy events. Solutions are not currently automated (since events with $M_I > 3.5$ are rare in Switzerland), but can be manually calculated and optimized within minutes of an event occurrence. Like the first-motion solutions, moment tensor solutions are also reported for significant earthquakes in the annual / bi-annual reports of the SED. The SED currently works on solutions to disseminate and visualize the existing first-motion and moment-tensor catalogs for public access.

In an attempt to further enrich the catalog of moment tensor solutions, the SED recently tested two methods based on waveform modeling (Sokos & Zahradnik, 2013; Heimann *et al.*, 2018), and a hybrid method (Kwiatek *et al.*, 2016) that combines amplitudes and P-wave polarities. For the waveform-based methods, we tested the algorithms for $M_I > 3.0$ earthquakes between 2019 to 2021. **Figure 2.5** shows the spatial distribution of the moment tensors computed using Grond for that time interval and by applying two 1D P- and S-wave velocity models for computing the Green's Functions. Overall, we were able to compute more moment tensors (~ 10) than the ones computed with the SeisComP module. The hybrid method allows to lower the magnitude of completeness for M_w and additionally to test the relationship between ML and M_w . In this respect, we computed moment tensors for all earthquakes that have a high-quality focal mechanism derived from P-wave polarities. The moment tensor solutions are mostly consistent with the focal mechanisms, and additional work is in progress in order to obtain a robust M_w that will allow to potentially implement the method in a near real time manner.

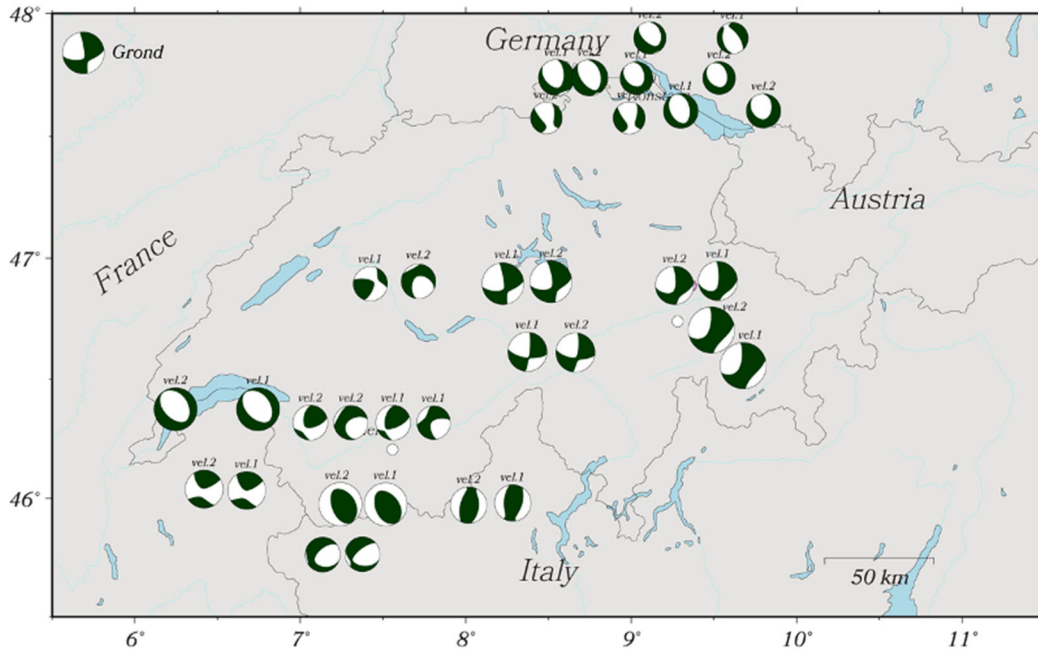


Figure 2.5. Moment tensor solutions for earthquakes recorded and located by the Swiss Seismological Service between 2019 and 2021. Solutions are computed using two 1D P- and S-wave velocity models (Diehl *et al.*, 2009; Diehl, Kissling, *et al.*, 2021), and the Grond software (Heimann *et al.*, 2018) for earthquakes with magnitude $2.9 \leq M_w \leq 4.2$.

2.6. Operational Double Difference Relocation

L. Scarabello, T. Diehl, J. Clinton

In order to assess the spatio-temporal evolution of natural and induced seismicity, real-time high-precision (relative) micro-seismic hypocenter locations are key information for understanding the situation and are preferred input in real-time applications like OEF or Advanced Traffic Light Systems (ATLS). From precise hypocenter locations, we can infer, for instance, the geometry and extent of a seismically active fault or the seismogenic volume affected by stimulation procedures. The spatio-temporal evolution of seismicity can be indicative for fluid-flow processes and allows first-order estimates on hydraulic properties as well as on the existence of possible hydraulic connections, which is crucial information especially to control induced seismicity. Precise and prompt information on spatial extent, geometries, and the spatio-temporal evolution of seismogenic structures can therefore enable near-real-time seismic hazard assessment of natural and induced seismicity.

This requires, however, relative relocations computed in near-real-time. Relative relocation procedures have been developed and introduced decades ago, but it is rare that these are applied in real time as a routine operation embedded in seismic network architectures. A strategy for such near-real-time relative relocation procedures has been developed at the SED, which has been implemented as a software

module, *scrtDD*⁸, that runs within SeisComP. The SED procedure follows the single-event *rtDD* strategy proposed by Waldhauser (2009) and uses waveform cross-correlation and double-difference methods to rapidly relocate new seismic events with high precision relative to past events with accurately known locations that comprise the background catalog. This background catalog is derived by a standard, multi-event double-difference relative relocation procedure (Waldhauser & Ellsworth 2000).

The *rtDD* method combines differential times derived from automatic as well as manual picks (once these become available after manual review). In addition, the waveforms of new events are automatically cross-correlated with those archived for nearby past events to measure accurate differential phase arrival times. The differential-time data are subsequently inverted to compute the single-event, relative location of a new event with respect to the double-difference background catalog. In addition, our *rtDD* implementation includes the possibility to generate a background catalog using the standard multi-event double-difference method.

Thanks to the integration of our *scrtDD* method into the SeisComP framework, it has been possible to establish a robust workflow around the standard SeisComP location modules in order to improve hypocenter precision in near real-time in Switzerland. Every automatic and manual origin in the SeisComP system is relocated in the single-event mode against the background catalog within a few seconds. Our *rtDD* method is also used for weekly updates of the double-difference background catalog throughout Switzerland, so that new events are continuously included. This is not only useful for providing up-to-date snapshots of high-resolution earthquake locations (multi-event relocation), but it is crucial for real-time, single-event double-difference relocations in regions of sparse background seismicity. Without an up-to-date background catalog, over time the real-time relocations might become inaccurate or even fail if attempted in areas of sparse background seismicity. **Figure 2.6.1** shows examples of seismic sequences in Switzerland, documenting the improvement in precision achieved by our multi-event double-difference procedure. Both single-event and multi-event relocation procedures are implemented in the operational monitoring system since 2021. Furthermore, concepts for more advanced visualization and dissemination of SED’s double-difference catalogs (single-event and multi-event) are currently being developed and tested.

⁸ Double-Difference relocation module: <https://github.com/swiss-seismological-service/scrtdd> (zenodo DOI 10.5281/zenodo.5337361)

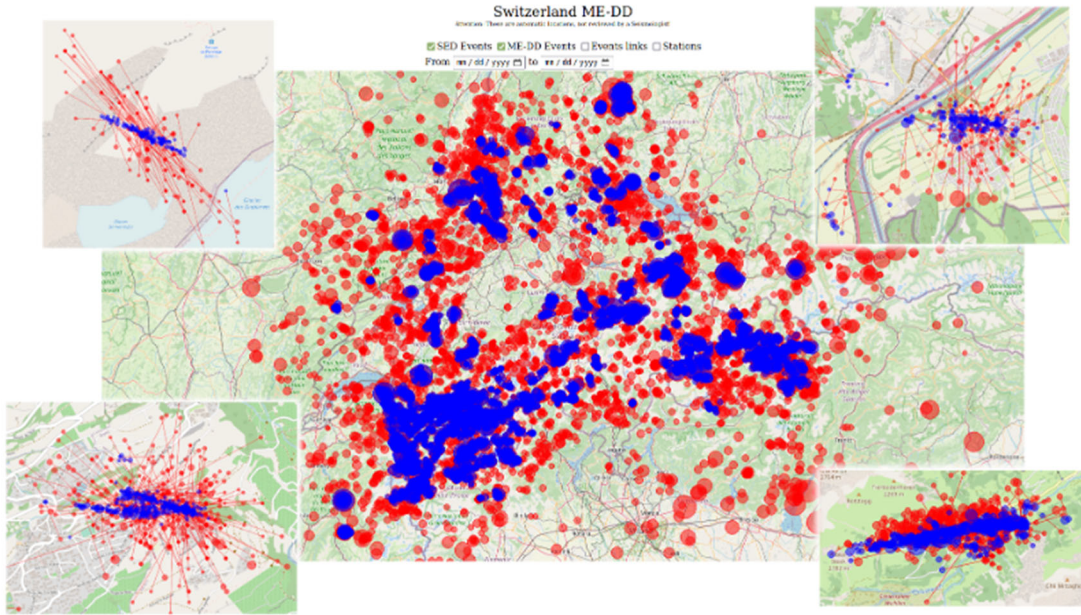


Figure 2.6.1. Examples of four seismic sequences in Switzerland, documenting the improvement in precision achieved by SED’s multi-event double-difference procedure (blue dots) in comparison with manual bulletin locations (red dots). Top left: Les Diablerets (VD/VS); top right: Balzers (FL); bottom left: St. Leonard (VS); bottom right: Elm (GL).

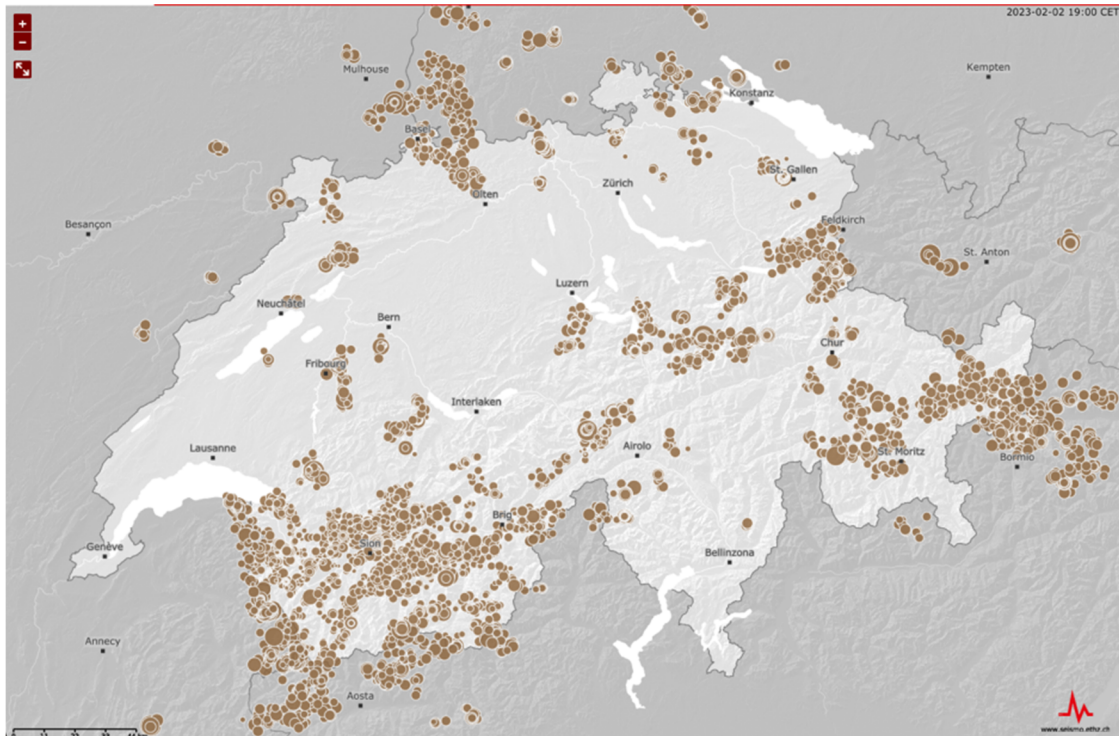


Figure 2.6.2. Map of Switzerland and surrounding area showing all seismicity relocated from the SED catalog since 2009. Refer to Figure 3 for a similar figure showing absolute locations.

2.7. Operational Template Matching

M. Mesimeri

In recent decades, computer capabilities and capacities have increased, and thus, computationally expensive methods, like waveform cross-correlation-based earthquake detection (template matching, or match filtered), have become a reality. Collecting enhanced earthquake catalogs in real time is of great importance for operational aftershock forecasting (OAF) (Mizrahi *et al.*, 2021) or real-time discrimination of earthquake sequences (Gulia & Wiemer, 2019). However, proposed methods for earthquake detection based on waveform cross-correlation are usually implemented offline and in a retrospective manner. An optimal case would be that the dedicated software is bound to the network real-time operations.

For this purpose, the SED has developed *SCDetect*⁹ (Mesimeri *et al.*, 2023; Armbruster *et al.*, 2022), an open-source SeisComP package written in C++, to detect earthquakes in real-time by applying template matching. Its highly configurable module, *scdetect-cc*, performs computationally efficient waveform cross-correlation in the time domain. The workflow (**Figure 2.7**) proposed here is fully compatible with the SeisComP architecture and modules. We define as *detector* (**Figure 2.7**) a run-time instance mapping the cataloged earthquake (referenced by its originID). A *detector-k* operates on a set of *templates*, which again map a continuous waveform-stream and a phase used for preparing the template waveform. An identical preprocessing is performed for the continuous waveforms and the template waveforms; it includes (i) filtering, (ii) resampling, and (iii) gap interpolation. Then, waveform cross-correlation takes place continuously as the data arrive and *local maxima* are computed. During the phase association stage, the *local maxima* extracted for each *template* are fed to the *detector's linker*, a matrix-based phase associator. After detecting and associating phases, *sc detect-cc* forwards messages to *scmaster*, SeisComP's messaging hub, with origins, picks, amplitudes, and magnitudes (**Figure 2.7**). Then downstream modules, namely *scevent*, associate the new origins and create unique events that are forwarded to the database and listed on other modules, for example *scolv*. Compatibility with SeisComP allows the user to leverage the SeisComP built-in GUI applications for visualizing the new detections, and, if desired, refine picks, relocate, and re-calculate magnitudes based on the local network configuration.

We applied the new software to past earthquake sequences in Switzerland and surrounding regions in order to evaluate its performance. For more “typical” mainshock-aftershock sequences, like the 2019 Bodanrück and the 2020 Elm sequences, we could detect at least all the cataloged earthquakes. By scanning only one station, we increased the number of detected earthquakes, however, these events are mostly not locatable, and the detections can only be used as time series (magnitude vs time). When

⁹ <https://github.com/swiss-seismological-service/scdetect> and <https://scdetect.readthedocs.io/en/stable/>

scanning more stations, the number of detections decreases, however, all detections have adequate phases and can be located.

We currently test *scdetect-cc* in real-time by scanning areas of high seismic activity in Switzerland, such as the Valais region. Multiple stations are scanned concurrently using templates from past sequences in the Valais (e.g. Anzere, 2019). With this configuration we are able to detect small magnitude earthquakes that are not detected by the operational pipelines. In addition, we evaluate the performance of *scdetect-cc* and its ability to communicate successfully with other SeisComP modules (such as *scrtDD*) and operational pipelines.

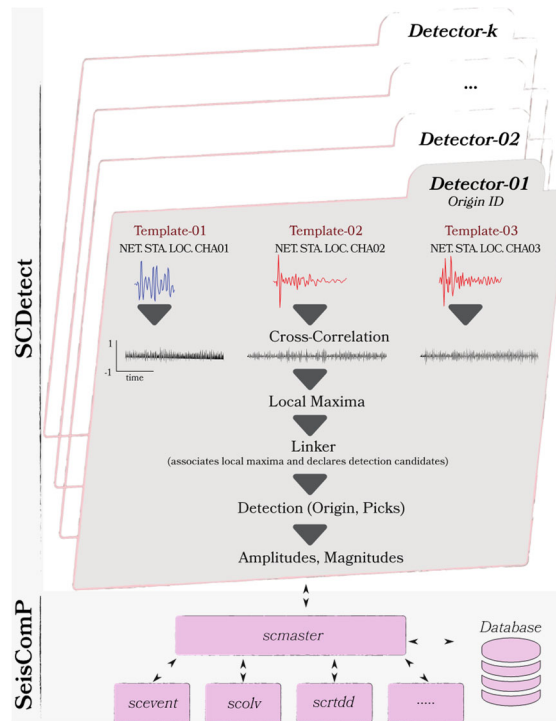


Figure 2.7. *scdetect-cc* workflow and how the module is implemented in the SeisComp monitoring framework.

2.8. ML Applications (WP2)

M.-A. Meier

Since around 2016, machine and deep learning methods applied to earthquake seismology are rapidly changing how scientists monitor seismicity, including at the SED. Before the widespread and successful use of deep learning in earthquake science, there used to be a trade-off between the quality and quantity of data products. Manually processed data products, such as seismicity catalogs, were typically of higher quality than their automated counter-parts. But they were necessarily of limited size. Now, state-of-the-art automated seismic processing methods reach a reliability and fidelity that rivals or even

surpasses that of human processing experts, and can be used to generate very large high quality data products, which form the basis of scientific studies. The SED has been pursuing multiple strands of research in deep learning-powered earthquake science, including for seismicity monitoring methods (both real-time and offline), planetary seismology, and seismicity forecasts.

We are working on implementing various existing machine learning models for seismic phase detection, arrival time estimation, signal/noise classification, phase association, and first motion polarity classifications. We use non-ML based methods in parallel as benchmarks, to identify where and to what extent the new methods improve monitoring performance. For all monitoring tasks we are planning to compare established, available models against new models that are trained from scratch, and against models that are transfer-learned using Swiss data.

An important aspect of these efforts is the implementation and testing of the machine learning methods at the various scales at which we monitor seismicity: from underground laboratory experiments (e.g., the [Grimsel Test Site](#), 10m scale; the [BedrettoLab](#), 100m scale), to geothermal reservoir scales (e.g., [Utah FORGE](#); 1-10km scale), to the national and regional monitoring scales (10-100s km). We have been working on deep learning-based methods on all these scales and are now targeting models that perform well at multiple scales simultaneously.

Our efforts include both classical monitoring module-based approaches (phase detection / picking / association / location etc.), as well as alternative waveform migration approaches such as MALMI (Shi *et al.*, 2022). We are simultaneously optimizing and comparing these algorithms in different observational settings, and work towards a fully optimized, general monitoring workflow.

In the context of the NASA InSight mission (Banerdt *et al.*, 2020) we have developed MarsQuakeNet (Dahmen *et al.*, 2022), a U-shaped convolutional neural network that uses observed spectrograms as input data to predict segmentation masks (**Figure 2.8**). These masks can effectively separate signal and noise components in the observed signals, allowing us to almost double the number of detections. Similar methods can potentially also be used to improve the detection sensitivity, and consequently, monitoring performance on Earth.

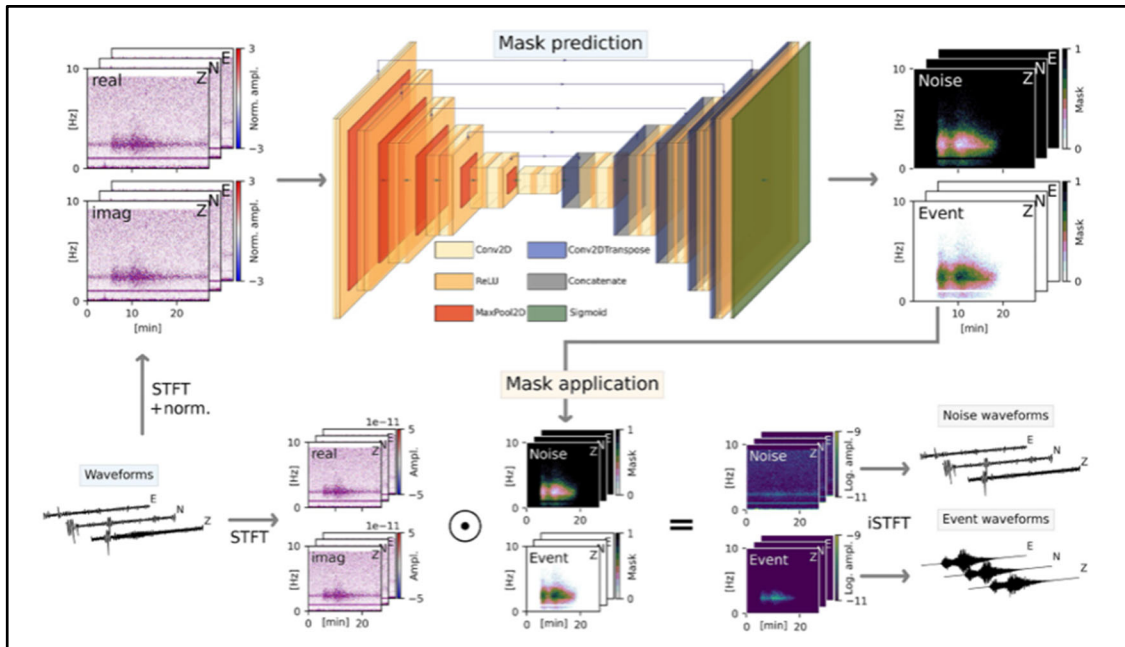


Figure 2.8. MarsQuakeNet method of Dahmen *et al.* (2022) for denoising seismic waveforms. The U-shaped convolutional neural network uses observed spectrograms as input data to predict segmentation masks that can effectively separate signal and noise components.

In tandem with the monitoring methods, we also develop, optimize, and compare innovative approaches to seismicity forecasting, which use catalogs of previous seismic activity as well as other observables as input parameters, to predict seismicity rates in space and time as an alternative to traditional OEF. This includes both deep learning models, as well as simpler methods, such as Lasso regressions. Such approaches are particularly interesting in induced seismicity setups, such as Utah FORGE and at the BedrettoLab, where forcing terms like injection pressures are known and can be used to explain the observed seismicity.

2.9. Site Response Analyses

P. Bergamo, D. Fäh

Mapping the local seismic response is one of the fundamental elements for seismic risk studies. Accurate models of local-scale amplification are generally performed in microzonation studies (e.g., Michel *et al.*, 2017; Hailemikael *et al.*, 2020). In comparison, for large-scale amplification models (e.g., national or European scale), the approach is generally more approximate, and frequently consists in mapping site response indicators (such as V_s30) using topographical and/or geological parameters as basis for the extrapolation (e.g. Vilanova *et al.*, 2018; Weatherill *et al.*, 2022).

To rigorously model the soil response in Swiss-wide risk modeling, at SED we have developed a national amplification model based on the direct mapping of *observed* local amplification at instrumented sites –

thus avoiding the indirect intermediate stage of charting soil condition proxies (such as Vs30). Cornerstone of the SED model is a dataset of site amplification functions derived for seismic stations of the Swiss networks by means of empirical spectral modeling (ESM, Edwards *et al.*, 2013; see **Figure 2.9a,b**). The ESM procedure has been routinely applied at SED for more than a decade; an empirical estimate of the soil amplification function is extracted from earthquake recordings after each event for all affected stations. By averaging the estimates over all the events recorded by a given station, we obtain a robust estimate of the local response of the hosting site as well as of its variability. The amplification functions refer to the same reference rock conditions defined by a generic Vs profile (Poggi *et al.*, 2011), which is used for all seismic hazard products in Switzerland. ESM-derived amplification functions are paired at SED stations with another type of key site metadata, i.e. the subsurface S-wave velocity profile and resonance characteristics as determined by in-situ geophysical measurements (SED site characterization database <http://stations.seismo.ethz.ch>, Fäh *et al.*, 2009; Michel *et al.*, 2014; Poggi *et al.*, 2017; Hobiger *et al.*, 2021).

For the production of the national soil amplification model, we selected the ESM amplification functions of (urban) free-field stations having acquired > 5 events (median is 50 events) with SNR > 3 between 2001-2021; the resulting dataset covers about 245 sites (**Figure 2.9a**), whose Fourier soil response functions were converted to pseudo-spectral acceleration (PSA) aggravation, for consistency with the common approach of earthquake engineering to use response spectra to define the seismic demand. The PGV, PSA(1.0s), PSA(0.6s), and PSA(0.3s) amplification factors measured at seismic stations were then interpolated over the national territory exploiting their proven correlation with layers of diffuse geological and morphological indicators (Bergamo *et al.*, 2019, 2021): a bespoke lithological classification (**Figure 2.9a**), multi-scale topographic slope and a national geological model of sediments' thickness (Swisstopo, 2019). We adopted the geostatistical interpolation scheme of regression kriging (Hengl *et al.*, 2007), which allows to consistently combine regressions between target (soil amplification) and predictor variables (site proxies) with local samplings of measured soil response at instrumented sites. The obtained amplification model (Bergamo *et al.*, 2022, 2023) consists of four soil response layers for PGV, PSA(1.0s), PSA(0.6s), and PSA(0.3s) (**Figure 2.9c**), with spatial resolution of 25 m; each layer is accompanied by its mapped site-to-site (φ_{S2S}) and single-site, within event-variabilities (φ_{SS}). The amplification maps for PGV and PSA at periods $T = 1.0$ and $T = 0.3s$ were additionally converted into layers of aggravation of macroseismic intensity using the relationships of Faenza & Michelini (2010, 2011); these maps are applied, for instance, in the SED ShakeMap® implementation (see section 3.3).

The national soil response model is complemented, for selected regions relevant from the hazard and/or risk point of view, by local amplification maps developed at SED for the urban areas of Visp (Panzer *et al.*, 2021, 2022), Sion (Perron *et al.*, 2022), Lucerne (Janusz *et al.*, 2022d), and Basel (Michel *et al.*, 2017). These smaller-scale models achieve a higher spatial resolution as they rely – for the prediction of soil response – on the ESM amplification functions and on dense networks of ambient vibration

measurements (hundreds of single-station acquisitions) or on a calibrated, comprehensive 3D geophysical-geological model for the Visp area.

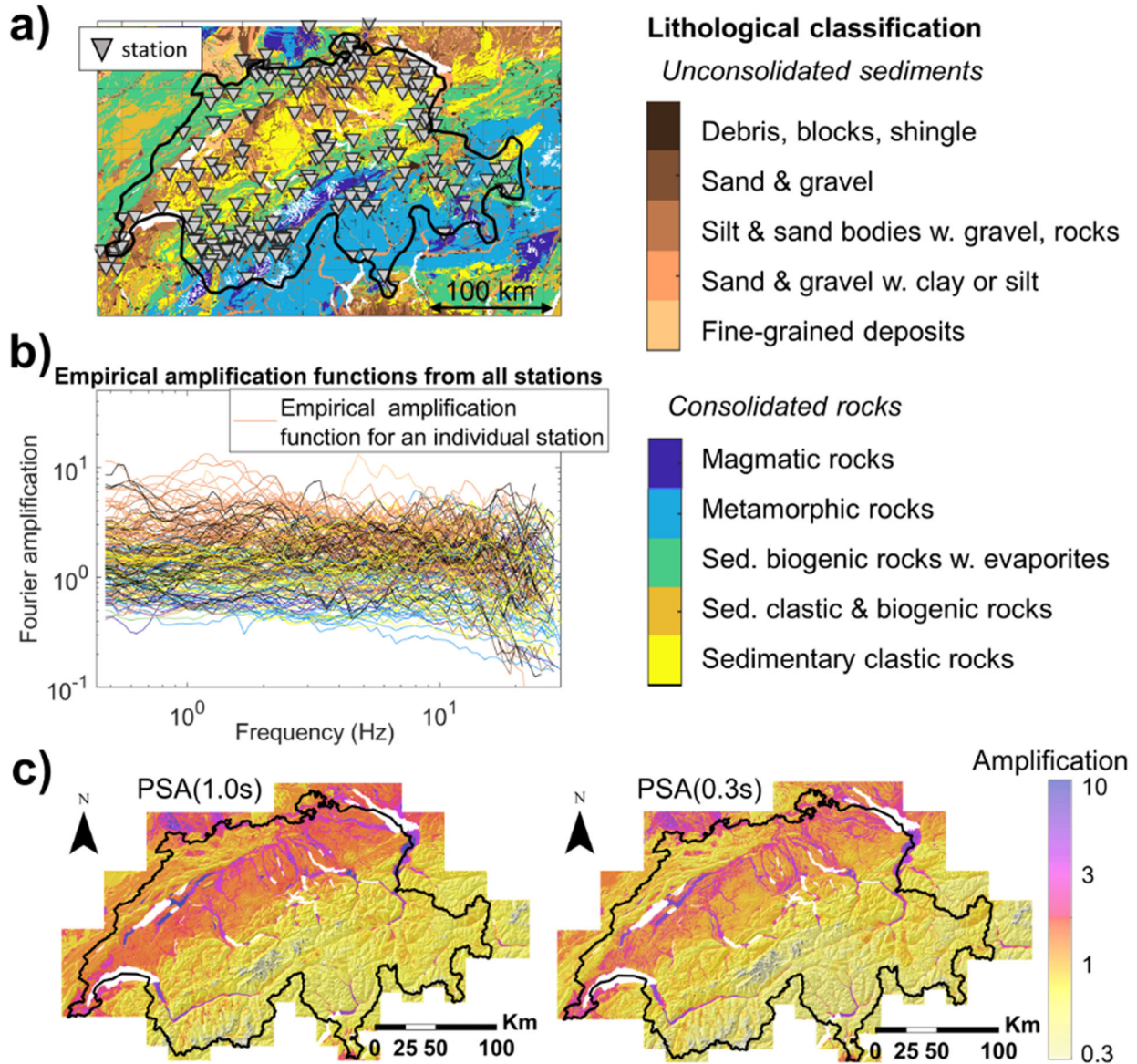


Figure 2.9. (a) Geographical locations of the ~245 (urban) free-field stations having recorded at least 5 earthquakes with SNR > 3 in the period 2000 – 2021, superimposed on the lithological classification of Switzerland employed to derive the national soil response model. (b) Empirical amplification functions derived for the stations in (a) by means of ESM; the color indicates the lithotype hosting the corresponding station. (c) PSA(1.0s) (left) and PSA(0.3s) (right) amplification maps (referred to $V_{s30} = 1105$ m/s), part of the national soil response model (Bergamo *et al.*, 2022, 2023).

2.10. Noise Interferometry

P. Sánchez-Pastor, A. Obermann

Seismic noise interferometry is based on the reconstruction of Green's functions from correlations of seismic noise records (e.g., Weaver & Lobkis 2001; Derode *et al.*, 2003; Campillo & Paul, 2003). Typically, ballistic waves are used for imaging the surface (e.g., Obermann *et al.*, 2016) and coda waves to monitor variations in the mechanical and structural properties in the crust (e.g., Sánchez-Pastor *et al.*, 2018). The main advantage of using seismic noise instead of earthquakes is the constant source of signals that can be recorded at any place on Earth. Therefore, the spatial resolution of seismic noise studies is mainly limited by the geometry and aperture of the seismic network (Stehly *et al.*, 2009).

Recently, the SED has started to apply noise interferometry to Switzerland. In order to quantify mechanical and structural changes in the crust, we are using the latest version of the Moving-Window Cross-Spectrum technique (MWCS, Brenguier *et al.*, 2014; Gómez-García *et al.*, 2018). This technique allows quantifying variations relative to the period under study without the need of defining a reference period. In Sánchez-Pastor *et al.* (2019) we have recently shown the potential of this technique to retrieve long-term variations that cannot be identified with other techniques such as *stretching* (Lobkis & Weaver, 2003; Sens-Schönfelder & Wegler, 2006).

In an initial feasibility study, we have started to reprocess seismic data for the time period 2019-2022 using stations within and near Switzerland equipped with broad-band sensors. We have retrieved surface waves at different frequency bands in order to sample different depths. The computational cost is expensive and the signal processing has been completed for a single frequency band at 0.1-0.5 Hz only. This band includes the secondary microseismic peak and Rayleigh waves are sensitive to depths between approximately 2 and 9 km. The depth sensitivity range is estimated from the computation of depth sensitivity kernels for Rayleigh waves using a 1D velocity model of Switzerland (Diehl *et al.*, 2021). In this frequency band, the speed of the Rayleigh waves has been estimated as 2.8 km/s. We have identified that the main noise sources come from the North Atlantic Ocean, which is in good agreement with previous studies performed in Europe (Lu *et al.*, 2022).

As an example, the results for three different station pairs are shown in **Figure 2.10**. As can be seen, the observed velocity changes time-series are formed by a combination of short- and long-term variations. In the long-term, some regions show a clear seasonal variation in the seismic velocities (**Figure 2.10b**) while others show a flatter time-series (**Figure 2.10b, d**). Those seasonal variations might be associated with changes in the seismic noise sources (Juretzek & Hadziioannou, 2016; Stutzmann *et al.*, 2009) and/or in the elastic properties of the crust. We are currently investigating the spatial distribution of the seasonal variations in Switzerland and trying to discriminate source-driven velocity variations from changes in the actual medium. We expect the latter might be correlated with the local seismicity. Furthermore, there is an increase in the seismic velocities starting in 2021 in some

areas (**Figure 2.10d**). This observation has been made in the southern part of Switzerland, in the Alpine region, and we suspect it might be related to slow tectonic processes.

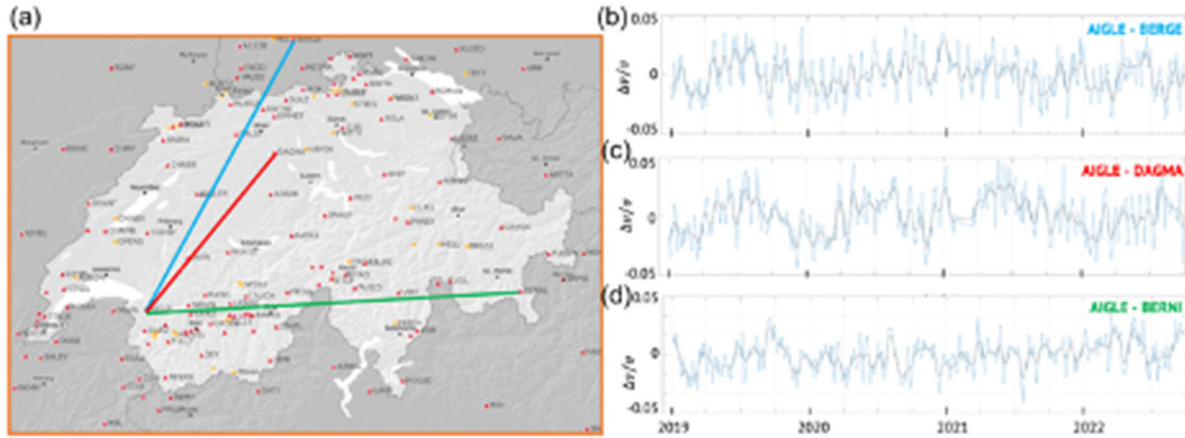


Figure 2.10. (a) Seismic station map in Switzerland. (b-d) Observed seismic velocity changes for the three seismic station couples indicated with solid lines in (a).

The SED is also working on the localization of the rapid seismic velocity changes with high temporal and spatial resolution. This requires a good data-quality control and analysis of the local noise sources in order to extract pure medium changes. Analyzing the spatio-temporal distribution of the velocity variations might help to understand the ongoing processes in the crust and compare it with the local and regional seismicity in the country.

Finally, coda wave based noise interferometry has great potential for the time-lapse monitoring of local engineering applications, such as dams, hydraulic stimulations, or carbon storage. Working with seismic data from the Basel and St. Gallen geothermal project sites, the SED observed tiny changes in seismic velocity and the waveform similarity (Obermann *et al.*, 2015; Hillers *et al.*, 2015). These aseismic responses of the subsurface to geomechanical well operations could have helped to recognize the unexpected reservoir dynamics at an earlier stage than the microseismic response alone. In preparation for potential Carbon Capture and Storage (CCS) sites in Switzerland, the SED is currently testing this method in Iceland.

2.11. Development of Integrated Seismic Real-time Stations (WP2)

L. Heiniger

Various applications in the context of a dynamic risk framework require input data from dense, real-time measurement networks to improve location accuracy, resolution, and magnitude of completeness. Even for site-characterization studies we nowadays often rely on real-time streaming mobile stations as

these can be permanently monitored to make sure that data is complete and campaign investments pay off.

In the past, mobile seismic stations were typically built from classic seismic components which have several disadvantages for use in dense, temporary networks. To enable data transmission in real time, a powerful data processing and transmission chain is necessary even at moderate sampling rates. However, traditional streaming-capable digitizers and industrial modems in particular, place high demands on the energy source and storage capacity. As a consequence, such mobile stations are usually 1-2 orders of magnitude heavier/larger than nodal-type sensors and are thus unsuitable for large-N deployments. Another limiting factor is the cost of such custom assemblies with traditional off-the-shelf components. Nodal type systems on the other hand are often limited with respect to bandwidth, dynamic range, and streaming capability.

In the context of RISE and related projects we developed a compact, fully integrated seismic real-time station that makes use of various emerging technologies to overcome these issues:

Data Communication: With the rise of IoT, new mobile network technologies have emerged. The recently introduced LTE Cat-M1 band is ideally suited for seismic data streaming in terms of bandwidth and power usage but commercial routers are only becoming available now. By integrating an early Cat-M1 module into our system we were able to reduce the power consumption for streaming by about 50% compared to traditional modems.

Data Processing: Linux systems offer a huge ecosystem of open-source tools for seismic data processing and transmission but have limited suitability for real-time tasks and typically require large amounts of energy compared to simple microcontrollers. We use a state-of-the-art ultra-low power System on Module (SOM) embedded in custom electronics to optimize power consumption and charging behavior.

Sensor & Digitizer: A compact 3-axis velocity sensor provides 10⁻⁵s–98⁰Hz bandwidth with a sensitivity of 1500⁻¹V/m/s.

Mechanical Design: A 3D printed inner frame provides stiff vertical coupling and allows the electronics to be removed in one piece. This greatly simplifies component access for assembly and maintenance. A clamping mechanism ensures adequate horizontal coupling. All external components (solar panel, GPS and LTE Antennas) are connected at the top.

Power: We ran solar power budget simulations to quantify power supply and storage requirements and designed a custom battery to maximize the use of the available space. By placing the battery below the frost line, we can use Lithium-Ion cells and do not have to rely on the temperature resilience of lead acid batteries. Current Li-Ion cells provide up to six times more energy density per kg compared to lead acid. Electronic battery management and passive safety features ensure safe operation even under harsh conditions.

The fully assembled sensor weighs less than 10kg and costs a fraction of a traditional mobile station. Initial field tests were conducted during the autumn and winter period of 2021/22 to assess performance, ease of deployment in various soils (using a hand auger), and power characteristics. While the results were promising (**Figure 2.11**), further testing will be required to provide a more systematic analysis of long-term power budgets and temperature behavior, as well as overall system performance. We are planning to manufacture a small batch series to conduct these tests. If results continue to meet our expectations, this newly developed sensor concept will potentially allow us to deploy much larger numbers of stations more rapidly and in more remote locations than what was possible in the past using traditional mobile assemblies.

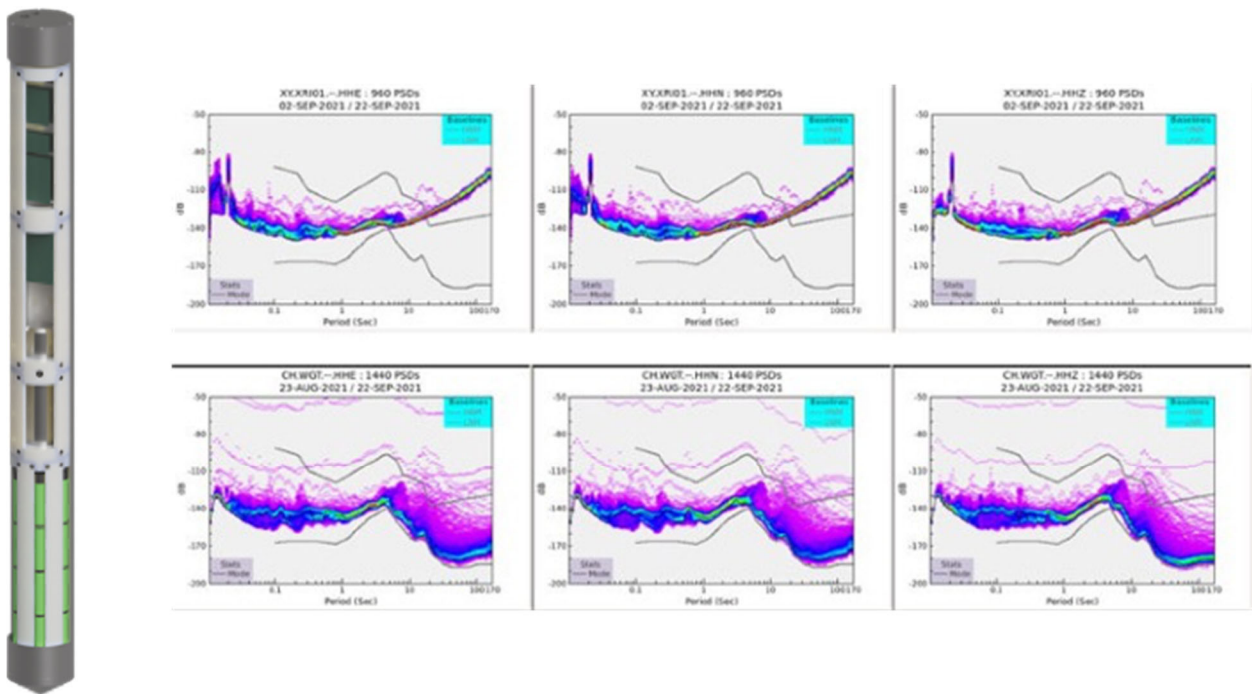


Figure 2.11. Left: Conceptual sensor drawing with electronics, sensor and battery (top to bottom). Right: Noise performance (top) compared to a permanently installed classic broadband station (bottom, Streckeisen STS-2 / Nanometrics Centaur). The PSD levels are comparable up to a period of around 6-7s.

3. Products & Services

3.1. Operational Earthquake (Loss) Forecasting (OEF & OELF) (WP3, WP4)

L. Mizrahi, M. Han, A. Papadopoulos

The SED is extending its approach to earthquake forecasting in Switzerland to complement the currently available time-independent (i.e. long-term) earthquake forecasts based on SUIhaz2015 (Wiemer *et al.*, 2016). Earthquakes tend to occur in clusters, leading to strong temporal fluctuations in their rate, which is not reflected in such long-term forecasts. The goal of the OEF project is to operationally provide updated earthquake probabilities, always considering the most recent as well as long-term data.

A few guiding principles for the development of the first Swiss time-dependent earthquake forecasting model include that it should be simple, consistent with the existing long-term earthquake forecasts of SUIhaz2015, and calibrated using Swiss data. Epidemic-Type Aftershock Sequence (ETAS) models (Ogata, 1988) are well suited for this task. They are being used or considered for OEF systems at several locations worldwide (Marzocchi *et al.*, 2014; Rhoades *et al.*, 2016; Field *et al.*, 2017; van der Elst *et al.*, 2022; Nandan *et al.*, 2021) and are the most extensively tested time-dependent models available (Woessner *et al.*, 2011; Ogata *et al.*, 2013; Strader *et al.*, 2017; Savran *et al.*, 2020). In ETAS, earthquakes are partitioned into background seismicity and aftershock clusters. This allows one to model background seismicity based on the SUIhaz2015 time-independent rate forecast, and the clustered seismicity using ETAS parameters that were calibrated on the local catalog.

Mizrahi *et al.* (in prep.) present the development and testing of multiple ETAS-based earthquake forecasting models for Switzerland. The simplest of these models only require a sufficiently large catalog of earthquakes as an input. More complex versions consider temporal variations in the completeness of the catalog, or additional information from the SUIhaz2015 model. **Figure 3.1.1** shows the fit to the Swiss catalog of inverted ETAS triggering laws in comparison to those inferred from Californian data.

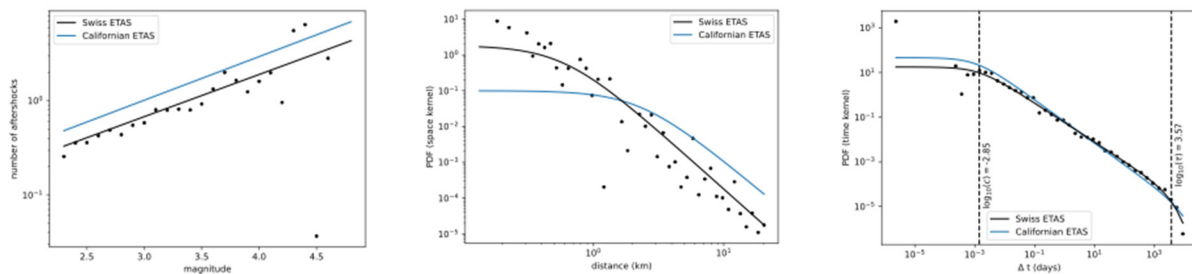


Figure 3.1.1. ETAS triggering laws calibrated on Swiss data, compared to those calibrated on Californian data, and compared to the observed triggering behavior in Switzerland. Observations are

plotted based on the inverted branching structure. From left to right: aftershock productivity, spatial aftershock density for a M 3.0 mainshock, temporal aftershock density. Inversion and visualization were done based on the code of Mizrahi *et al.*, 2023.

All models are tested using pseudo-prospective forecasting experiments and retrospective consistency tests. Because large earthquakes happen rarely in Switzerland and the catalog is complete at low magnitudes only since a few decades, significant differences in-between the models' performance are not identifiable due to the lack of a larger sample size. The benefit of time-dependent models is however evident: probabilities can vary by several orders of magnitudes between quiet times and during aftershock sequences (see **Figure 3.1.2**). Furthermore, in the experiments of Mizrahi *et al.* (in prep.), all tested time-dependent models show a clear information gain over the null (time-independent) model during the most seismically active periods.

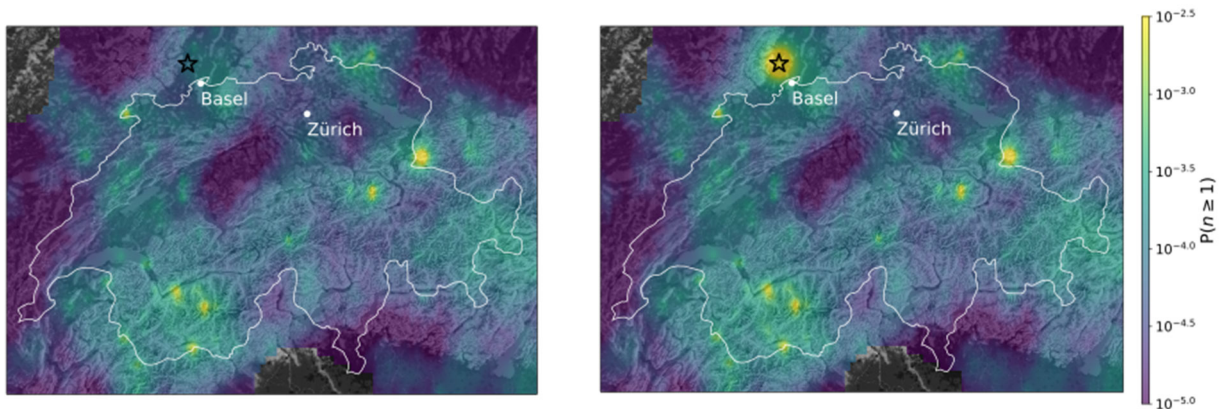


Figure 3.1.2. Probability of one or more earthquakes with $M \geq 2.5$ to occur within the next 7 days, shortly before the occurrence of the M 4.7 Mulhouse event in September 2022 (left), and 5 minutes afterwards (right). The probability in Basel increased by a factor of more than 100.

Besides the forecasting model itself, the SED is also developing an operational system which produces updated earthquake forecasts in real time, which will initially be used internally and later made available to the public and government agencies. A critical aspect to consider in such a system is how information is communicated to the public. This topic has been addressed within the RISE project (Dallo *et al.*, 2020; Dallo *et al.*, 2022; Dryhurst *et al.*, 2021) and the results of this work form the basis on which the SED's OEF dashboard is developed. Moreover, the SED is working on providing not only short-term earthquake probabilities, but also the associated seismic hazard and loss, factoring in the transiently increased earthquake rate. This will form an Operational Earthquake Loss Forecasting (OELF) module, building upon the OEF and ERM-CH23 (see section 1.3) efforts. The updated earthquake rate forecast will feed into ERM-CH23, and be used to obtain a short-term view of earthquake risk that will be updated at appropriate intervals. Loss forecasts are likely to provide more actionable information to individuals, public authorities, and other stakeholders.

3.2. Earthquake Early Warning (EEW) (WP4, WP5)

M. Böse, F. Massin, J. Clinton, D. Jozinović

For around a decade, the SED has been developing methods and open-source software for EEW implemented in set of SeisComP (Hanka *et al.*, 2010) modules, which together form the ETHZ-SED SeisComP EEW (ESE) system (Massin *et al.*, 2021; **Figure 3.2a**). The Virtual Seismologist (VS) and Finite-Fault Rupture Detector (FinDer) algorithms form the core of ESE. The VS (Cua, 2005) provides rapid EEW magnitudes building on existing SeisComP detection and location modules for point-source origins. FinDer (Böse *et al.*, 2012; 2023), by contrast, matches growing patterns of observed high-frequency seismic acceleration amplitudes with modeled templates to identify fault rupture extent, and hence can infer independently on-going finite-fault rupture in real-time. Together these methods increase the tolerance to failures of a single algorithm, while providing EEW for all event magnitudes. To combine the independent algorithm estimates in a probabilistic manner while suppressing false alerts, the SED is currently developing a Decision module (Jozinović *et al.*, 2023), adapting the approach outlined in Minson *et al.* (2017). Source parameter estimates from both VS and FinDer are used to predict ground motion envelopes at a set of stations which are then compared to the observed values.

In Switzerland, VS and FinDer are used for testing and demonstration, not for public alerting. The two algorithms are similarly fast and often produce first EEW alerts within 4–6 s of event origin (Massin *et al.*, 2021). The VS method utilizes phase picks to provide fast locations and magnitudes for any event that is detected by the national network. Since 2014, the median delay for the first VS alert has been 8.7 s (56 earthquakes, $2.7 \leq M \leq 4.6$). FinDer, on the other hand, is activated when peak amplitudes exceed a certain threshold (here 2 cm/s^2 at 3 neighbored stations), typically for larger earthquakes with magnitudes greater than 3.5. However, earthquakes as small as M2.7 have been detected. The median delay for the first FinDer alert since 2017 has been 7 s (10 earthquakes $2.7 \leq M \leq 4.3$). These delays are smaller than those observed in Central America, where the SED is testing messaging to pilot users using ESE within the ATTAC (Alerta Temprana de Terremotos en América Central) project, and where first alert delay times range from 10–15 s for shallow on-shore seismicity, and between 20–25 s for off shore or deep events (Massin *et al.*, 2020; Porrás *et al.*, 2021). Also in the United States West Coast ShakeAlert EEW system (Given *et al.*, 2018), which adopts FinDer for public alerting since 2018, delays are typically a bit longer (median delay of 8.5 s), largely due to a more conservative trigger criterion (Böse *et al.*, 2023).

The SED continues to optimize the Swiss Seismic Network for EEW. Today over 175 permanent stations include strong motion stations, and the majority of stations have been upgraded to include low-latency streaming. Station uptime is high. The median value for the travel time of the P-waves from event origin to the fourth station accounts for 3.5 s of delay; with an additional 1.4 s (+1.2 s, -0.3 s) for data sample delays in real-time testing. Alert delays can be decreased by network densification. However, using a stochastic earthquake catalog, which samples the earthquake rate forecast of the Swiss Hazard Model, and adopting a simple consequence model to relate predicted intensities to losses, Böse *et al.* (2022)

demonstrated that the impact of additional stations for EEW in Switzerland is limited. For a repeat of the 1356 M6.6 Basel earthquake large areas of Switzerland would be affected by strong to very strong shaking and could obtain positive warning times outside a 30 km-wide blindzone (**Figure 3.2b**).

While large earthquakes in Switzerland are rare and warning times generally short, a recent public survey shows that 70% of the Swiss population would like rapid notifications for all earthquakes that are felt, even if they have a low damage potential (Dallo, Marti, Clinton, *et al.*, 2022). Possible platforms for mass notifications in Switzerland are the MeteoSwiss or AlertSwiss apps, which can receive and display push notifications on mobile devices, or - once available in Switzerland - through cell broadcast.

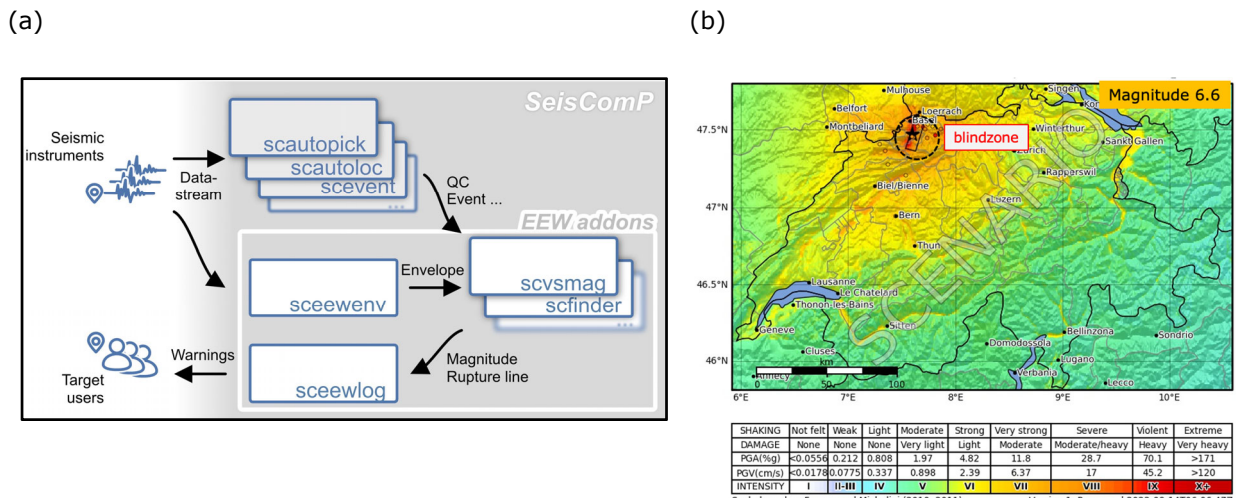


Figure 3.2. (a) Schematic workflow of the SED-ETHZ SeisComP EEW (ESE) system (from Massin *et al.*, 2021). The main SeisComP framework includes automatic picking and location modules (*scautopick* and *scautoloc*) which can be tuned for event detection with P-wave arrival detection at four stations. The VS algorithm is implemented in the *scvsmag* module. FinDer is a stand-alone library that is integrated in the *scfinder* wrapper module. SeisComP event detections are fed into VS together with acceleration and displacement envelope amplitudes (provided by the *sceewenv* module), while FinDer uses peak acceleration values. Both algorithms provide EEW to target users via the *sceewlog* module using multiple real-time dissemination interfaces, including the EEW Display (EEWD) open-source client software (Cauzzi *et al.*, 2016) and Firebase Cloud Messaging (Moroney, 2017). (b) Theoretical EEW performance of ESE during a repeat of the M6.6 Basel earthquake considering the current seismic data availability offered by the Swiss seismic network. Assuming peak ground motion moveout and rupture velocities slower than S-wave velocity, areas outside of the 30 km-wide blindzone could obtain positive warning time.

3.3. ShakeMaps

C. Cauzzi

Among the SED earthquake products, ShakeMap® (usgs.github.io/shakemap; Worden *et al.*, 2020), has been in use in Switzerland for about 15 years. ShakeMap® is a well-known scientific and technical framework that maps rapid (i.e., within minutes of an earthquake occurrence) seismic shaking

information based on recorded and predicted intensity measures [peak ground acceleration (PGA) and peak ground velocity (PGV)], 5%-damped pseudo-acceleration spectral ordinates (PSA) and macroseismic intensity levels, including amplification due to local site effects. The SED ShakeMap framework has been regularly updated since the original implementation (Cauzzi *et al.*, 2015) to exploit and integrate the latest advances in seismic monitoring, seismic hazard and engineering seismology at the SED, as well as core software improvements. SED ShakeMaps are constrained by the real-time records of about 400 permanent and temporary stations acquired by the SED.

Event and waveform parameterization is performed using the software module *scwfparam* (Cauzzi *et al.*, 2016) part of the free open-source SeisComP distribution. SED ShakeMaps use Swiss-specific ground-motion models (Cauzzi *et al.*, 2015; Edwards *et al.*, 2016) included in OpenQuake (Pagani *et al.*, 2014), the ground-motion to intensity conversion equations of Faenza and Michelini (2010, 2011), and high-resolution site amplification models (Bergamo *et al.*, 2022) that allow accurate and reliable estimates of ground shaking across the Swiss alpine and northern foreland regions. Automatically collected and processed felt intensities are overlain on SED ShakeMaps for comparison; though currently these are not automatically integrated in the calculations.

The SED maintains an archive of instrumental ShakeMaps for events (presently ~700, see e.g. **Figure 3.3a**) with magnitude larger than 2.5 occurred since 1991, as well as an atlas of large historical ShakeMaps (Cauzzi *et al.*, 2018, see **Figure 3.3b**) constrained by the intensity observations included in ECOS-09 (Fäh *et al.*, 2011). For internal SED use, SED ShakeMaps provide input to estimate the likelihood of earthquake-triggered mass-movements (landslides, rockfalls) for significant events (M4.5+) following the empirical model and procedure of Cauzzi *et al.* (2018) that calculates the probability of occurrence of such earthquake-induced effects through a set of geospatial susceptibility proxies and peak ground acceleration (**Figure 3.3c**).

There are plans to include rapid finite-fault information in SED ShakeMaps, provided by the FinDer (Böse *et al.*, 2012) algorithm already operating in real time at SED. SED ShakeMaps are also used as input to rapid loss assessment in the framework Earthquake Risk Model for Switzerland. The SED is a core founder and contributor of the European ShakeMap initiative (shakemap.eu.ingv.it) that promotes international collaboration and harmonization of ShakeMap procedures in the greater European region.

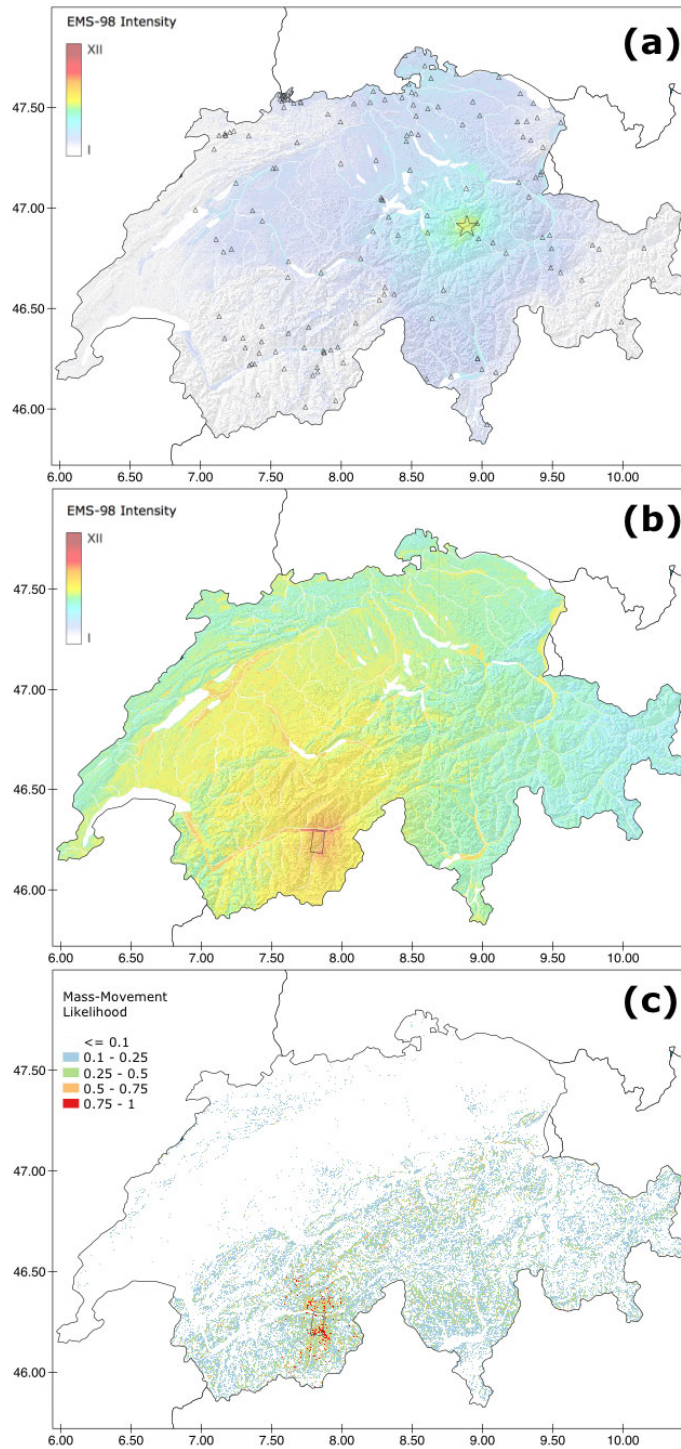


Figure 3.3. (a) Instrumental SED ShakeMap for the earthquake occurred near Linthal on 2017-03-06 at 20:12:07 UTC (Mw ~4.3), triangles = seismic stations, star = epicenter; (b) SED atlas ShakeMap for the possible repetition of the 1855 Stalden-Visp earthquake (Mw ~6.2), rectangle = surface projection of the possible causative fault; (c) mass-movement likelihoods for the earthquake in (b).

3.4. Rapid Impact Assessment (RIA) (WP4)

A. Papadopoulos, L. Danciu

The destructive potential of an earthquake is highly dependent on its size, its proximity to the built environment, as well as various regional factors. Numerous impact indicators (i.e., earthquake characteristics, ground shaking, and earthquake intensity) are often readily accessible in the aftermath of an earthquake, especially in regions with dense and high-quality networks of seismic stations. In Switzerland, the SED has been using the ShakeMap codes since 2007 to provide nation-wide maps of ground motion and macroseismic intensity, following any local earthquake with local magnitude $M_L \geq 2.5$ (section 3.3). The recent development of ERM-CH23 (section 1.3) allows extending SED's near real-time post-earthquake products even further.

Rapid impact assessment (RIA) describes the computational framework, developed within the SED, to quantify the effects of an earthquake, immediately after its occurrence. RIA is intended to offer first-order information to the public and help decision makers prioritize resources and organize the emergency response. Similar systems have been previously proposed and/or operated at continental (ELER, Erdik *et al.*, 2010) or global (PAGER, Wald *et al.*, 2011) scale.

The Swiss RIA system is based on OpenQuake's scenario calculator (Pagani *et al.*, 2015) and is set to accept ShakeMap rather than ground motion models as input (see **Figure 3.4**). In a nutshell, a ShakeMap is generated once an earthquake is located and its magnitude is estimated by the seismic network. The RIA Calculator will be activated when the ground shaking map is available. Monte Carlo simulations are used to generate multiple ground motion field realizations at the location of the building assets in the underlying ERM-CH23 exposure model. The simulated ground motion values are used in conjunction with the vulnerability functions associated with each asset to sample damage and loss estimates.

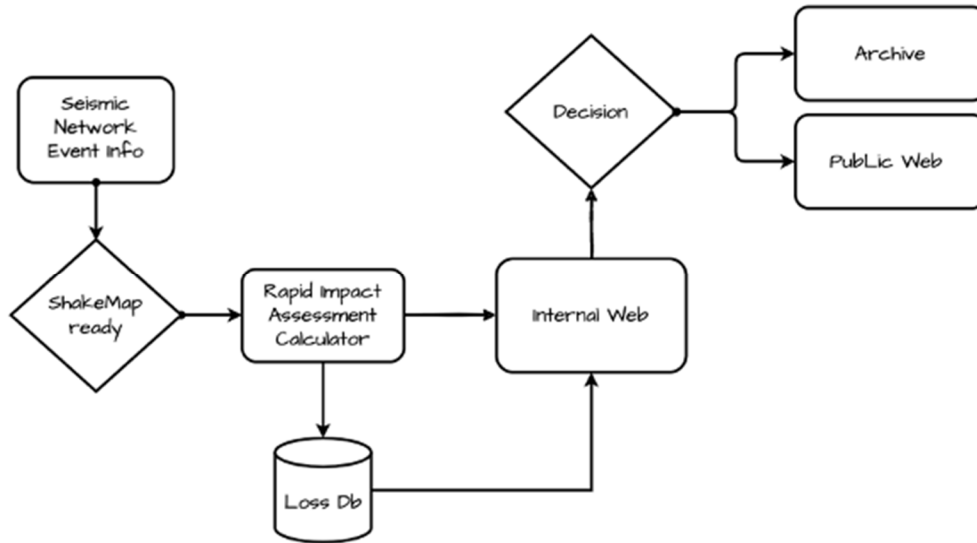


Figure 3.4. Flowchart describing the operational Rapid Impact Assessment (RIA).

In Switzerland, the operational RIA will provide rapid estimates of various loss types (damage, direct economic loss, injuries, deaths, population in need of shelter) aggregated at the national, cantonal, and municipal level. These results are compiled in a standardized template (more on the communication products, section 4.2) that depicts diverse information such as a map of ground shaking, as well as visualizations that communicate loss at different scales, along with any associated uncertainty. The results may be disseminated internally for sanity checks, publicly for general audience, or archived. The RIA system will be fully integrated and operational with the seismic network operations, and near-real-time calculations will be triggered for every magnitude $M > 3.0$ earthquake detected within a certain radius around and within Switzerland.

3.5. Structural Health Monitoring (SHM) (WP3)

Y. Reuland, P. Martkis, E. Chatzi

Due to the slow retrofit and replacement rates of existing buildings, the slow uptake of modern earthquake resistance standards, and even the sheer aspect of the intensity of certain of these extreme events, earthquakes continue to threaten the integrity of the built environment and thus, trigger large-scale post-earthquake inspections. Not all buildings react in the same way to earthquake actions and thus, a rapid understanding of the extent of damage to buildings and its consequences on providing safe shelter for the population is a crucial contribution to an earthquake-resilient Europe. Current post-earthquake integrity assessment of buildings relies on expert-conducted visual inspections that, despite being increasingly standardized, suffer from possible subjectivity and delay recovery. However, recent advances in sensor development offer reliable sensing hardware at lower costs, thus rendering broad monitoring of conventional buildings, or a sufficient number of characteristic samples thereof, a realistic outlook.

Structural health monitoring (SHM) offers the tools to analyze such a permanent inflow of sensor data and retrieve information regarding the structural state (health) of the structure. In the absence of direct evidence of building damage, indicators of damage need to be derived from indirect measurements, with accelerations forming the primary means to such an end. Damage-sensitive features (DSFs) can be extracted from continuous measurements and contribute to the detection and localization of earthquake-induced damage (Reuland *et al.*, 2023; Reuland *et al.*, 2022). In addition, data-driven classification schemes may be employed for near-real-time data-driven building tagging (Reuland *et al.*, 2021). However, the scarcity of real-world dynamic monitoring data of healthy and, above all, damaged structures hinder a direct application of machine-learning methods to data-driven damage diagnostics. Thus, the quantification of damage and its consequences on the seismic capacity of the earthquake-damaged building require complementary input from engineering models. Several approaches to overcome this limitation have been developed at the Chair of Structural Mechanics and Monitoring at ETH Zurich, within the context of RISE:

- SHM-based fragility functions, that relate probabilities of a structure to reach a given damage-state to DSFs, have been formulated (Reuland *et al.*, 2021; 2022). Monitoring the building behavior has the potential to improve upon current fragility functions that formulate damage probability with respect to ground-motion intensity and may provide near-real-time damage tags (see **Figure 3.5**).
- A machine-learning methodology, relying on domain adaptation, has been successfully used to transfer a damage-state classification from simulated training data, obtained with a parametrized engineering model that could further benefit from model order reduction (Agathos *et al.*, 2022), to real measurements stemming from experimentation (Martakis *et al.*, 2023). With this methodology, only healthy data, which can be collected through standard instrumentation under operational conditions, is required from real-world structures.
- To ensure that sensors are functional and record valuable data during earthquakes, a framework for automated detection of faulty sensors has been developed (Martakis *et al.*, 2022a).
- Finally, in addition to rapid post-earthquake damage assessment, monitoring data have the potential to contribute to earthquake preparedness by reducing the uncertainty and regional variability of capacity curves that are used to derive fragility functions. This uncertainty has been tested with data from nine measured buildings in the Zurich area (Martakis *et al.*, 2022b) by using a new testing approach to record shaking data of buildings during demolitions, which exceeds typical ambient vibration levels (Martakis *et al.*, 2020).

- After successfully testing seismic SHM on individual buildings, the application of SHM-based rapid loss assessment has been integrated into a regional demonstrator (Nievas *et al.*, 2023). Integrating monitoring data and engineering models into a robust framework will pave the way to make SHM-based real-time building tagging operational.

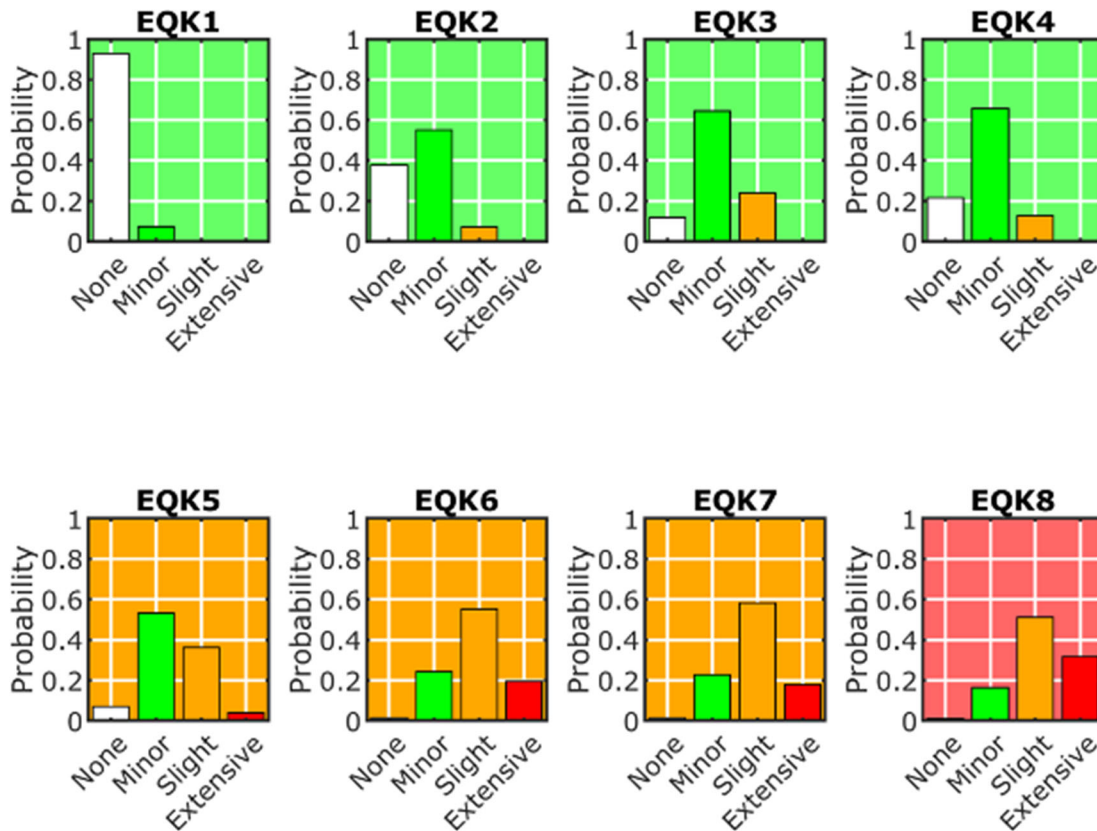


Figure 3.5. Prediction of post-earthquake building tag probabilities for eight ground motions of a building tested on a shake table by Beyer *et al.* (2015). Based on the combination of damage probabilities derived with SHM-based fragility curves for three DSFs, a tag is attributed (corresponding to the background color of the subplots) (Reuland *et al.*, 2022).

3.6. Recovery and Rebuilding Efforts (RRE) (WP4)

N. Blagojevic, L. Bodenmann, Y. Reuland, B. Stojadinovic

Resilient communities are characterized by their capacity to swiftly recover from extreme events. While retrofitting actions decrease the earthquake risk and, consequently, reduce the efforts required to repair buildings after a damaging earthquake, rapid recovery is essential to a quick restoration of the communities' functions. By reducing the downtime of buildings and infrastructure systems, rapid recovery reduces negative social and economic impacts. Regional recovery models and resilience

assessment tools simulate recovery trajectories of the built environment, enabling what-if analyses that can guide decision-makers towards effective resilience-improving actions. In addition, ex-ante analyses may improve disaster preparedness by establishing resource quantities required for a swift community recovery and by supporting the creation of post-earthquake recovery plans that contain procedures to be followed to minimize building downtime. The iRe-CoDeS framework, developed at the Chair of Structural Dynamics and Earthquake Engineering at ETH Zurich (Blagojević *et al.*, 2022a), offers the capacity to perform such analyses. The framework simulates regional recovery of buildings and interdependent infrastructure systems and provides outputs that allow for risk-based assessment of community resilience goals (Blagojević *et al.*, 2022a). As part of the RISE project, OpenQuake software for regional hazard and risk assessment has been interfaced with iRe-CoDeS, adding recovery as a new layer of capabilities on top of the existing seismic risk and seismic hazard layers (Reuland *et al.*, 2022).

Early loss assessment is often incomplete and imprecise, which undermines efficiency and speed of public and private stakeholder responses. Reliable information on the regional severity of damage is a crucial enabler of well-organized emergency responses and recovery efforts, which affect immediate disaster assistance as well as the long-term recovery. To assist crucial decision-making, further complicated by intense time pressure, we proposed to dynamically update regional post-earthquake damage estimates. Gaussian Process inference models are used to fuse available early inspection data with a pre-existing earthquake risk model (Bodenmann *et al.*, 2022). The continuous inflow of inspection data is leveraged to reduce the uncertainty in the geographic distribution of ground shaking intensity and to improve regional building damage estimates by simultaneously updating all the components of regional loss assessment (Bodenmann *et al.*, 2021), as shown in **Figure 3.6** using a simulated M5.8 earthquake occurring near Zurich, Switzerland.

Combining regional recovery and resilience assessment tools with a framework to reduce the uncertainties of regional loss assessment allows for a reduction of the uncertainty in recovery trajectories. Uncertainties stem from stochastic earthquake simulations, numerous assumptions related to the seismic performance of structures and the state of the community at the time of the event, as well as the assumptions related to the post-earthquake repair, institutional recovery strategy and the behavior of the people residing in the community. These uncertainties can be reduced by updating the regional recovery models using the early inspection information (Blagojević *et al.*, 2022c). Thus, what-if analyses can be conducted in real-time to inform decision-makers on the state of the community during its recovery and on the optimal deployment of community resources for the remaining of the recovery efforts to ensure a swift community recovery, minimizing the post-earthquake unmet demand of community inhabitants for resources they need in their everyday lives.

If an iRe-CoDeS model is available to stakeholders for ex-ante evaluation of resilience goals, they can re-use when an earthquake occurs to update it with the early inspection information. Thus, such a

framework may help in delivering recommendations on the organization of recovery efforts and on the remaining recovery time.

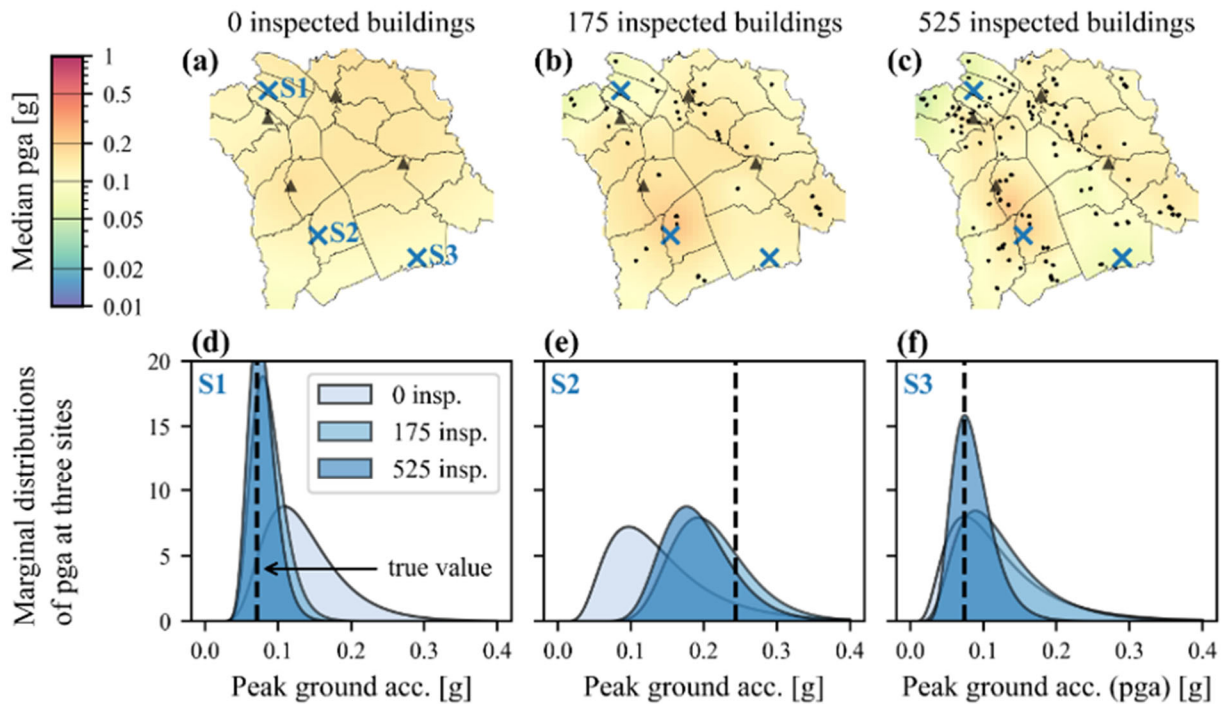


Figure 3.6. Simulated M5.8 earthquake in Zurich (Bodenmann *et al.*, 2021): Inferred estimates of PGA from shake map and using early inspection data of 175 and 525 buildings, respectively. The top row (a-c) shows maps of the median PGA inferred from inspection data, while the bottom row (d-f) illustrates the posterior distributions of PGA for three specific sites, defined in (a).

4. Operation & Communication

4.1. Operation, IT (WP8)

P. Kästli, Nicholas

Our progress on operational dynamic risk services is summarized in RISE Deliverable 8.4.

4.2. Communication & Societal Perspective (WP5, WP8)

I. Dallo, M. Marti, N. Valenzuela

The SED, as a federal agency, has the mandate to inform the Swiss public, authorities, and the media about earthquakes, and to provide warnings. To this end, the SED has established a clearly defined communication chain with event-specific products (**Figure 4.2**), and has developed static products that are available on its website www.seismo.ethz.ch (e.g., hazard map, and behavioral recommendations).

Regarding event-related communication, the SED monitors ground shaking 24/7 days a week. Within approximately 90 seconds after an event, details about the time, location, magnitude, and possible effects are published on the website. When an earthquake with a magnitude of 2.5 or higher occurs, federal and cantonal authorities are informed automatically. In addition, details about the earthquake are posted on Twitter in the three national languages plus English, as well as on the Swiss multi-hazard *AlertSwiss* and *MeteoSwiss* platforms. From a magnitude 3 on, an email is sent to a list of journalists/news portals informing them about the event. Every recorded earthquake is assessed by a SED standby team (“Pikett”) that takes further actions if needed and is available for media requests. These about 30 employees, who have previously been trained (e.g., yearly media training), are ready within one hour, so that key positions can be staffed rapidly in an emergency. A more detailed description of the communication chain is available in Luoni *et al.* (2021).

In quiet times, the SED is also active in science communication to transfer knowledge about earthquakes and related topics to those interested (e.g., news articles, information materials, direct exchange such as the *Scientifica*).

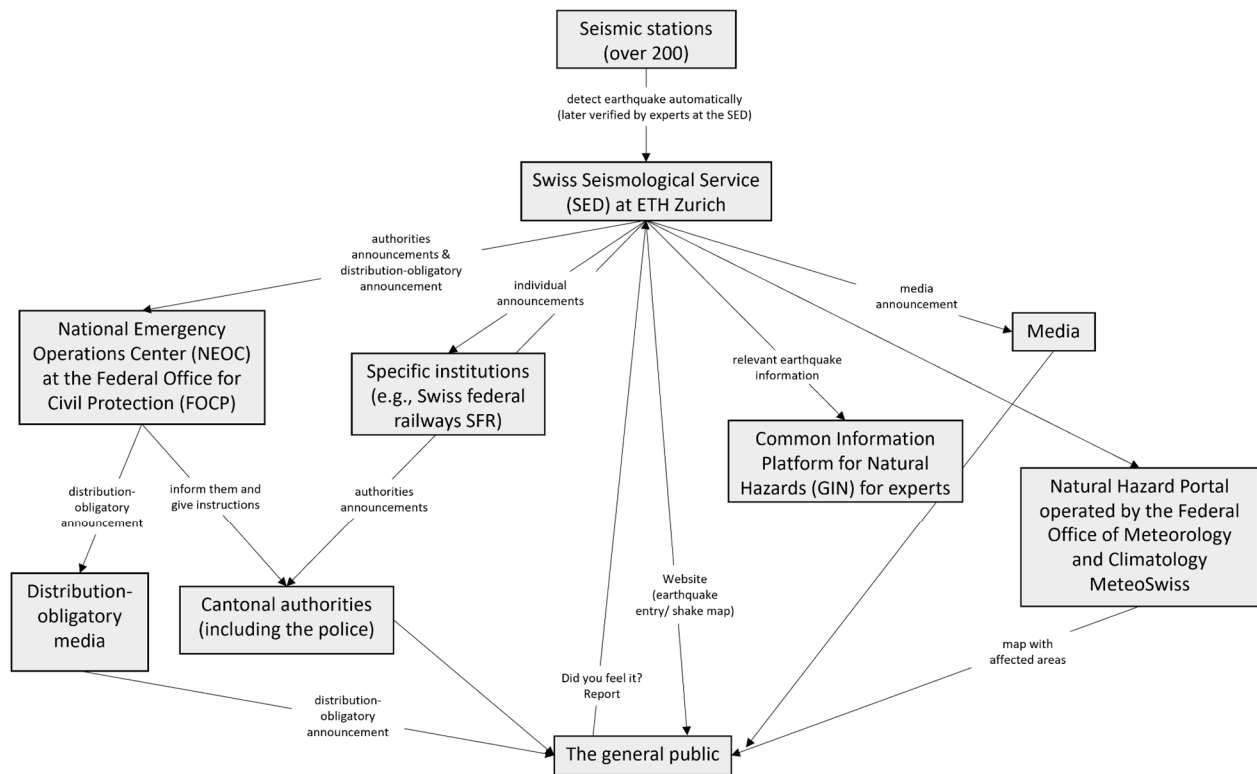


Figure 4.2. Communication pathways for seismic information in Switzerland.

To ensure that the above described communication chain is effective, end-users' needs, expectations, and skills have to be taken into account (Hobbs & Rollins, 2019). Therefore, the SED continuously interacts with various societal stakeholders to involve them in the product development and, consequently, tailor them to their needs (Lang *et al.*, 2012; Melles *et al.*, 2012). In the last few years, the SED has co-developed and evaluated various information products.

Maps are a common means to communicate spatial hazards or risk to society. However, although preferred by them, many people struggle to correctly interpret maps. Marti *et al.* (2019) thus tested the Swiss seismic hazard map versions with the public and professional societal stakeholders. The study has shown that (i) people are able to distinguish between high hazard and low hazard regions; (ii) moderate hazard regions are not perceived as endangered; (iii) the word 'within' is correctly understood when communicating probabilities of a certain event within a certain time period; and (iv) '60% probability for a damaging earthquake' is interpreted by the public as 'quite plausible or almost certain'.

Since seismic risk assessments have significantly improved in the last few years, there is a shift from hazard to risk communication, which should increase societies' preparedness and disaster resilience. The SED has been testing various outputs of the first publicly available Earthquake Risk Model of Switzerland (ERM-CH23) with professional stakeholders of the society and the general public. Marti *et al.* (2022) showed that people and professionals consider RIA reports and risk scenarios to be very important. Further, to depict the uncertainties of the model estimates, the most simple visualization using ranges only was best understood and most liked (Marti *et al.*, 2022). Thus, histograms currently used in existing outlets need to be reconsidered. Another insight was that professional stakeholders and the public were similarly challenged to correctly interpret the information provided (Marti *et al.*, 2022). The SED also tested the first Swiss earthquake risk map with a public survey to assess people's design preferences, correct interpretation of the information provided on the map, and intention to take protective actions based on the risk information. Thereby, the SED benefits from its experiences in supporting the release of the first openly available European Seismic Risk Model (ESRM20) (Crowley *et al.*, 2021; EFEHR, 2022).

To better understand how to communicate earthquake information on multi-hazard platforms, three online surveys with different experiments and virtual focus groups were conducted (Dallo, 2022; Dallo, Marti, Valenzuela Rodríguez, *et al.*, 2022). The main results indicate that people prefer (i) a combination of visual and textual information, i.e. single map with more detailed information beneath (Dallo *et al.*, 2020); (ii) a combination of pictorial and textual behavioral recommendations (Dallo *et al.*, 2020); (iii) interactive features such as push notifications, a sharing function, or an 'I'm safe' button (Dallo & Marti, 2021); (iv) that data privacy issues are considered (Dallo & Marti, 2021); (v) messages with a time indication and action-keywords because these indications increase their understanding of the information and intention to take the recommended actions (Dallo, Stauffacher, *et al.*, 2022); and (vi) that the icon of the epicenter and the person's location must be clearly distinguishable (Valenzuela

Rodríguez, 2021). Further, a study showed that gray background is interpreted as 'no data is available' and not that there are no current earthquake notifications (Valenzuela Rodríguez, 2021).

Past earthquakes have shown that disseminated misinformation led to panic and anxiety and, consequently, triggered inappropriate behaviors (Flores-Saviaga & Savage, 2020; Mero, 2019; Peary *et al.*, 2012). The SED, together with international partners, thus started a project to explore misinformation and, more precisely, the most common earthquake myths. Outcomes of this collaboration are (i) a Communication Guide for institutions responsible for public communication (Dallo, Corradini, *et al.*, 2022); (ii) an opinion paper discussing the relevance of addressing earthquake myths especially for seismologists (Fallou *et al.*, 2022); and (iii) a research article providing insights regarding expert opinions about the myths (Dryhurst, Mulder, *et al.*, 2022). The insights of these three efforts have been key for the SED to be better prepared to avoid the spread of misinformation.

So far, EEW alerts are not sent to the Swiss public. However, the assessment of the public's preferences for EEW systems and alert designs which push people to take protective actions provided relevant insights into the societal perspective (Dryhurst *et al.*, 2021). These findings will allow decision-makers to define system boundaries and settings in the future. The main insights from a public survey in Switzerland conducted by the SED (Dallo, Marti, Clinton, *et al.*, 2022) are: (i) the Swiss public wants to receive EEW alerts for all felt events; (ii) the system preferences are similar to the preferences in other countries; (iii) EEW alerts with pictograms push people the most to take actions; and (iv) what people like best is not necessarily what motivates them to take action.

Regarding OEF communication, the SED has collaborated with the Winton Center at the University of Cambridge and tested OEF communications with the general public in Italy, Switzerland, and California in the US. The survey, among others, revealed that (Dryhurst, Dallo, *et al.*, 2022): (i) people in all three countries gave similar answers except that Swiss people had a lower forecast risk perception; (ii) maps representing OEF probabilities as different colored isoline compartments mislead the public; and (iii) the best information combination is a geographical map showing the forecast area, textual information about the current, absolute chance of an earthquake (e.g., out of 100,000 towns with exactly this chance, we would expect...), and a risk ladder to give context. Currently, a testing concept for Swiss-specific communication outputs is in development.

All the above-mentioned studies further showed that people's personal factors influence their correct interpretation of the information provided, design preferences, and perceived usefulness. Therefore, these factors should also be considered when designing information campaigns. Key for information campaigns is the regular communication, the consideration of the context, the choice of the right channel, the training of risk communicators, and community-based approaches (Marti *et al.*, 2020). A challenge is to fulfill end-users' wish to receive personalized notifications at the same considering their

concerns about data privacy. Overall, it is important to build an interdisciplinary expert group to design communication products and then test them with relevant end-users before releasing them publicly.

5. Conclusions & Outlook

M. Böse, all

The SED is creating a user-centered dynamic risk framework for Switzerland that considers earthquake hazard and risk as integrated and dynamically evolving over time. Over the past decade, the SED has improved the seismic observation capabilities throughout Switzerland through implementation of denser sensor arrays and advanced data processing. These advancements enhance earthquake forecasting (OEF), early warning (EEW), and rapid impact assessment tools (RIA). The newly developed National Earthquake Risk Model of Switzerland (ERM-CH23), which will be publicly released in March 2023, is anticipated to increase public awareness of earthquake risk in Switzerland, help authorities update their risk assessments and implement mitigation measures, serve as a scientific reference, and aid the insurance industry. It will also serve as the foundation for rapid impact assessment (RIA) and operational earthquake loss forecasting (OELF) by the SED. These systems will not only provide crucial real-time information after damaging earthquakes, facilitating rapid response and decision making of disaster managers who have to allocate resources, but will also provide information to the general public supporting them to better understand what happened and what might happen next.

A key element of the integration of risk products enabled by RISE is the harmonization of all products in seamless products that refer to the same databases, workflows and software. Another key innovation of our products enabled by RISE is the focus on user needs, building on quantitative social science tools, such as online surveys and focus groups (WP5). For example, the rapid impact assessments for Switzerland that we now operate (**Figure 5**) use the same ShakeMap provided in near real-time, which uses the same site amplification layers derived for the national risk models, the impact on people and building is computed based on the national databases of buildings and their vulnerability, and for computing rapid impact we use Openquake for scenario products, rapid impact assessment, and probabilistic products. OEF calculations use the hazard and risk model used for long-time hazard and risk calculation and for RIA products. The visual representation of the rapid impact we designed based on feedback from focus groups and discussions with stakeholders at the federal and cantonal levels, including new visualizations of uncertainties. This harmonization of products and workflows across different applications is key to wide adaptation and universal recognition of products, it also allows synergies to be maximised.

simultaneously optimizing and comparing these algorithms in different observational settings, and working towards a fully optimized, general monitoring workflow.

- The SED continues to test noise interferometry techniques to quantify mechanical and structural changes in the crust. The subsurface's aseismic response to geomechanical well operations could reveal unexpected reservoir dynamics. The SED is currently testing this technique in Iceland in preparation for potential Carbon Capture and Storage (CCS) sites in Switzerland.
- The SED continues to test its new sensor concepts with the goal of deploying larger numbers of stations faster and in more remote locations than traditional mobile assemblies.

The SED also continues to further advance its risk-products:

- The SED aims to offer short-term earthquake probabilities and related seismic hazard and loss, taking into account temporarily increased earthquake rates, thus creating an OELF module building on OEF and ERM-CH23.
- The SED aims at providing rapid earthquake information and (actionable) EEW to the Swiss public. Platforms for mass notifications in Switzerland could be the MeteoSwiss or AlertSwiss apps. Cell broadcasting is not yet available and legally allowed in Switzerland.
- SED ShakeMaps will provide input into rapid loss assessment for the ERM-CH23. The SED is planning to add rapid finite-fault information to ShakeMaps using output from the EEW system.
- The SED aims at integrating the RIA system into seismic network operations and thus initiating near-real-time calculations for earthquakes in and around Switzerland above magnitude 3.0.
- The SED will continue its efforts towards cost-benefit analysis/multi-criteria analysis of various risk products.

The SED has a well-established communication network to provide rapid earthquake information over multiple channels to the society; thus fulfilling society's primary information needs. Research about how to communicate earthquake forecasts is key but has also brought up some challenges: (i) people struggle to interpret small probabilities, (ii) it is not trivial to find a balance between complexity and comprehension; and (iii) end-users (including civil protection and the general public) do not know what to do with the information. More efforts are thus needed on how to integrate OEF into the current dynamic risk communication framework and on how to best support the translation from probabilities into actions.

6. References

- Agathos, K., Tatsis, K. E., Vlachas, K., & Chatzi, E. (2022). Parametric reduced order models for output-only vibration-based crack detection in shell structures. *Mechanical Systems and Signal Processing*, 162, 108051.
- Armbruster, D., M. Mesimeri, P. Kaestli, T. Diehl, F. Massin, and S. Wiemer (2022). SCDetect: Near Real-Time Computationally Efficient Waveform Cross-Correlation Based Earthquake Detection during Intense Earthquake Sequences. EGU GA 2022. <https://doi.org/10.5194/egusphere-egu22-12443>
- Baer, M., Deichmann, N., Fäh, D., Kradolfer, U., Mayer-Rosa, D., Rüttener, E., Schler, T., Sellami, S., Smit, P., 1997. Earthquakes in Switzerland and surrounding regions during 1996. *Eclogae Geologicae Helvetiae* 90(3), 557-567.
- Banerdt, W.B., Smrekar, S.E., Banfield, D., Giardini, D., Golombek, M., Johnson, C.L., Lognonné, P., Spiga, A., Spohn, T., Perrin, C. and Stähler, S.C. (2020). Initial results from the InSight mission on Mars. *Nature Geoscience*, 13(3), pp.183-189.
- Bergamo P, Hammer C, Fäh D (2019) SERA deliverable D7.4: Towards improvement of site condition indicators. <https://doi.org/10.3929/ethz-b-000467564>
- Bergamo P, Hammer C, Fäh D (2021) Correspondence between Site Amplification and Topographical, Geological Parameters: Collation of Data from Swiss and Japanese Stations, and Neural Networks-Based Prediction of Local Response. *Bulletin of the Seismological Society of America* 112(2):1008–1030
- Bergamo P, Panzera F, Cauzzi C, Glüer F, Perron V, Fäh D (2022). A national ground motion amplification model for Switzerland based on site proxies and incorporating local response observations at instrumented sites. 3rd European Conference on Earthquake Engineering & Seismology, Bucharest, Romania, 4th – 9th September 2022.
- Bergamo P et al. (2023). A site amplification model for Switzerland based on site-condition indicators and incorporating local response as measured at seismic stations. Submitted to *Bulletin of Earthquake Engineering*.
- Beyer, K., Tondelli, M., Petry, S., & Peloso, S. (2015). Dynamic testing of a four-storey building with reinforced concrete and unreinforced masonry walls: prediction, test results and data set. *Bulletin of Earthquake Engineering*, 13(10), 3015–3064.
- Blagojević, N., Hefti, F., Henken, J., Didier, M., & Stojadinović, B. (2022a). Quantifying disaster resilience of a community with interdependent civil infrastructure systems. *Structure and Infrastructure Engineering*, 0(0), 1–15. <https://doi.org/10.1080/15732479.2022.2052912>
- Blagojević, N., Didier, M., & Stojadinović, B. (2022b). Quantifying component importance for disaster resilience of communities with interdependent civil infrastructure systems. *Reliability Engineering & System Safety*, 228, 108747. <https://doi.org/https://doi.org/10.1016/j.res.2022.108747>
- Blagojević, N., Bodenmann, L., Reuland, Y., & Stojadinović, B. (2022c). Validating A Regional Recovery Model: The Case of 2010 Kraljevo Earthquake (In Review).
- Blagojević, N., Hefti, F., Henken, J., Didier, M., & Stojadinović, B. (2022d). Quantifying disaster resilience of a Reuland, Y., Bodenmann, L., Blagojevic, N., & Stojadinovic, B. Deliverable 4.4 Development of RRE forecasting services in OpenQuake.
- Bodenmann, L., Reuland, Y., & Stojadinović, B. (2022). Dynamic post-earthquake updating of regional damage estimates using Gaussian processes. <https://doi.org/10.31224/2205> (In review)
- Bodenmann, L., Reuland, Y., & Stojadinović, B. (2021). Dynamic updating of building loss predictions using regional risk models and conventional post-earthquake data sources. 31st European Safety and Reliability Conference (31ESREL), Angers, France.
- Böse, M., T. H. Heaton, and E. Hauksson (2012). Real-time Finite Fault Rupture Detector (FinDer) for large earthquakes, *Geophysical Journal International*, 191, no. 2, 803–812, doi: 10.1111/j.1365-246X.2012.05657.x.
- Böse, M., A. N. Papadopoulos, L. Danciu, J. F. Clinton, and S. Wiemer (2022). Loss-based Performance Assessment and Seismic Network Optimization for Earthquake Early Warning, *Bull. Seismol. Soc. Am.* 112 (3): 1662–1677, <https://doi.org/10.1785/0120210298>.
- Böse, M., J. Andrews, R. Hartog, and C. Felizardo (2023). Performance and Next-Generation Development of the Finite-Fault Rupture Detector (FinDer) within the United States West Coast ShakeAlert Warning System, *Bull. Seismol. Soc. Am.* XX, 1–16, doi: 10.1785/0120220183
- Bonilla, L. F., Archuleta, R., & Lavallée, D. (2005). Hysteretic and dilatant behavior of cohesionless soils and their effects on nonlinear site response: Field data observations and modeling. *Bulletin of the Seismological Society of America*, 95, 2373–2395
- Braunmiller, J., N. Deichmann, D. Giardini, S. Wiemer. 2005. Homogeneous Moment-Magnitude Calibration in Switzerland. *Bulletin of the Seismological Society of America*, Vol. 95, No. 1, pp. 58, doi: 10.1785/0120030245
- Brenguier, F., Campillo, M., Takeda, T., Aoki, Y., Shapiro, N. M., Briand, X., et al. (2014). Mapping pressurized volcanic fluids from induced crustal seismic velocity drops. *Science*, 345(6192), 80–82. <https://doi.org/10.1126/science.1254073>
- Burjánek J. et al., 2018. Ambient vibration characterization and monitoring of a rock slope close to collapse. *Geophysical Journal International*, 212(1), 297–310
- Burjánek, J., Kleinbrod, U., & Fäh, D., 2019. Modeling the Seismic Response of Unstable Rock Mass With Deep Compliant Fractures. *Journal of Geophysical Research-Solid Earth*, 124(12), 13039-13059. doi:10.1029/2019jb018607
- Campillo, M., Paul, A., 2003. Long-range correlations in the diffuse seismic coda. *Science* 299 (5606), 547–549. <https://doi.org/10.1126/science.1078551>.
- Cauzzi, C. Y. Behr, J. Clinton, P. Kästli, L. Elia, and A. Zollo (2016). An Open-Source Earthquake Early Warning Display. *Seismological Research Letters*. 87, pp. 737–742

- Cauzzi, C., D. Fäh, D. J. Wald, J. Clinton, S. Losey, and S. Wiemer (2018). ShakeMap-based prediction of earthquake-induced mass movements in Switzerland calibrated on historical observations, *Natural Hazards*, 92, no. 2, 1211–1235, doi: 10.1007/s11069-018-3248-5.
- Cauzzi, C., R. Sleeman, J. Clinton, J. D. Ballesta, O. Galanis, and P. Kästli (2016). Introducing the European Rapid Raw Strong-Motion Database, *Seismological Research Letters*, 87, no. 4, 977–986, doi: 10.1785/0220150271.
- Cauzzi, C., B. Edwards, D. Fäh, J. Clinton, S. Wiemer, P. Kästli, G. Cua, and D. Giardini (2015). New predictive equations and site amplification estimates for the next-generation Swiss ShakeMaps, *Geophysical Journal International*, 200, no. 1, 421–438, doi: 10.1093/gji/ggu404.
- Crowley, H., Dabbeek, J., Despotaki, V., Rodrigues, D., Martins, Silva, V., Romão, X., Pereira, N., Weatherill, G., & Danciu, L. (2021). European Seismic Risk Model (ESRM20) [EFEHR Technical Report 002 V1.0.0]. Eucentre. <https://doi.org/10.7414/EUC-EFEHR-TR002-ESRM20>
- Cua, Georgia B. (2005) Creating the Virtual Seismologist: Developments in Ground Motion Characterization and Seismic Early Warning. Dissertation (Ph.D.), California Institute of Technology. Doi: 10.7907/M926-J956. <https://resolver.caltech.edu/CaltechETD:etd-02092005-125601>
- Dahmen, N.L., Clinton, J.F., Meier, M.A., Stähler, S.C., Ceylan, S., Kim, D., Stott, A.E. and Giardini, D., 2022. MarsQuakeNet: A more complete marsquake catalog obtained by deep learning techniques. *Journal of Geophysical Research: Planets*, 127(11), p.e2022JE007503.
- Dallo, I. (2022). Understanding the communication of event-related earthquake information in a multi-hazard context to improve society's resilience [Doctoral dissertation]. ETH Zurich.
- Dallo, I., Corradini, M., Fallou, L., & Marti, M. (2022). How to fight misinformation about earthquakes? - A Communication Guide. <https://doi.org/10.3929/ethz-b-000530319>
- Dallo, I., & Marti, M. (2021). Why should I use a multi-hazard app? Assessing the public's information needs and app feature preferences in a participatory process. *International Journal of Disaster Risk Reduction*, 57, 102197. <https://doi.org/10.1016/j.ijdr.2021.102197>
- Dallo, I., Marti, M., Clinton, J., Böse, M., Massin, F., & Zaugg, S. (2022). Earthquake early warning in countries where damaging earthquakes only occur every 50 to 150 years – The societal perspective. *International Journal of Disaster Risk Reduction*, 83, 103, <https://doi.org/10.1016/j.ijdr.2022.103441>
- Dallo, I., Marti, M., Valenzuela Rodríguez, N., & Stauffacher, M. (2022). Improving earthquake information in a multi-hazard context (Society: Data Gathering and Information Sharing with the Public and Policy-Makers) [Deliverable]. European Horizon-2020 project RISE.
- Dallo, I., Stauffacher, M., & Marti, M. (2020). What defines the success of maps and additional information on a multi-hazard platform? *International Journal of Disaster Risk Reduction*, 49, 101761. <https://doi.org/10.1016/j.ijdr.2020.101761>
- Dallo, I., Stauffacher, M., & Marti, M. (2022). Actionable and understandable? Evidence-based recommendations for the design of (multi-)hazard warning messages. *International Journal of Disaster Risk Reduction*, 74, 102917. <https://doi.org/10.1016/j.ijdr.2022.102917>
- Deichmann, N., Baer, M., Braunmiller, J., Dörfli, D.B., Bay, F., Delouis, B., Fäh, D., Giardini, D., Kastrup, U., Kind, F., Kradošfer, U., Kunzle, W., Rothlisberger, S., Schler, T., Salichon, J., Sellami, S., Spuhler, E., Wiemer, S., 2000b. Earthquakes in Switzerland and surrounding regions during 1999. *Eclogae Geologicae Helvetiae* 93, 395–406.
- Derode, A., Larose, E., Tanter, M., de Rosny, J., Tourin, A., Campillo, M., Fink, M., 2003. Recovering the Greens function from field-field correlations in an open scattering medium (L). *J. Acoust. Soc. Am.* 113, 2973. <https://doi.org/10.1121/1.1570436>, 10, 11, 12, 114.
- Diehl, T., S. Husen, E. Kissling, and N. Deichmann (2009). High-resolution 3-D P-wave model of the Alpine crust, *Geophys. J. Int.* 179, no. 2, 1133–1147, doi: 10.1111/j.1365-246X.2009.04331.x.
- Diehl, T., N. Deichmann, J. Clinton, P. Kästli, C. Cauzzi, T. Kraft, Y. Behr, B. Edwards, A. Guilhem, E. Korger, et al. (2015). Earthquakes in Switzerland and surrounding regions during 2014, *Swiss J. Geosci.* 108, no. 2–3, 425–443, doi: 10.1007/s00015-015-0204-1.
- Diehl, T., T. Kraft, E. Kissling, and S. Wiemer (2017). The induced earthquake sequence related to the St. Gallen deep geothermal project (Switzerland): Fault reactivation and fluid interactions imaged by microseismicity, *J Geophys Res Solid Earth*, 122, no. 9, 7272–7290.
- Diehl, T., J. Clinton, N. Deichmann, C. Cauzzi, P. Kästli, T. Kraft, I. Molinari, M. Böse, C. Michel, M. Hobiger, et al. (2018). Earthquakes in Switzerland and surrounding regions during 2015 and 2016, *Swiss J. Geosci.* 111, no. 1–2, 221–244, doi: 10.1007/s00015-017-0295-y.
- Diehl, T., J. Clinton, C. Cauzzi, T. Kraft, P. Kästli, N. Deichmann, F. Massin, F. Grigoli, I. Molinari, M. Böse, et al. (2021a). Earthquakes in Switzerland and surrounding regions during 2017 and 2018, *Swiss J. Geosci.* 106, no. 3, 543–558, doi: 10.1007/s00015-013-0154-4.
- Diehl, T., E. Kissling, M. Herwegh, and S. Schmid (2021b). Improving Absolute Hypocenter Accuracy with 3D Pg and Sg Body-Wave Inversion Procedures and Application to Earthquakes in the Central Alps Region, *J. Geophys. Res. Solid Earth*, 1–26, doi: 10.1029/2021jb022155.
- Diehl, T., H. Madritsch, M. Schnellmann, T. Spillmann, E. Brockmann, and S. Wiemer (2023). Seismotectonic evidence for present-day transtensional reactivation of the slowly deforming Hegau-Bodensee Graben in the northern foreland of the Central Alps, *Tectonophysics*, 846, 229659, doi: 10.1016/j.tecto.2022.229659.
- Dreger, D. S. (2003). 85.11 TDMT_INV: Time domain seismic moment tensor INVersion, *Int. Geophys.* 81, no. PART B, 1627, doi: 10.1016/S0074-6142(03)80290-5.

- Dryhurst, S., Dallo, I., Luoni, G., Marti, M., & Freeman, A. L. J. (2022). Field evaluation of OEF communications (Society: Data Gathering and Information Sharing with the Public and Policy-Makers) [Deliverable]. European Horizon-2020 project RISE.
- Dryhurst, S., Luoni, G., Dallo, I., Freeman, A. L. J., & Marti, M. (2021). Designing & implementing the seismic portion of dynamic risk communication for long-term risks, variable short-term risks, early warnings (Society: Data Gathering and Information Sharing with the Public and Policy-Makers) [Deliverable]. European Horizon-2020 project RISE.
http://static.seismo.ethz.ch/riser/deliverables/Deliverable_5.3.pdf#page=56&zoom=100,92,948
- Dryhurst, S., Mulder, F., Dallo, I., Kerr, J. R., McBride, S. K., Fallou, L., & Becker, J. S. (2022). Fighting misinformation in seismology: Expert opinion on earthquake facts vs. fiction. *Frontiers in Earth Science*, 10. <https://www.frontiersin.org/articles/10.3389/feart.2022.937055>
- Edwards B, Michel C, Poggi V, Fäh D (2013). Determination of Site Amplification from Regional Seismicity: Application to the Swiss National Seismic Networks. *Seismological Research Letters* 84(4):611-621.
- Edwards, B., C. Cauzzi, L. Danciu, and D. Fäh (2016). Region-Specific Assessment, Adjustment, and Weighting of Ground-Motion Prediction Models: Application to the 2015 Swiss Seismic Hazard Maps, *Bulletin of the Seismological Society of America*, 106, no. 4, 1840–1857, doi: 10.1785/0120150367
- Edwards, B., B. Allmann, D. Fäh, and J. Clinton (2010). Automatic computation of moment magnitudes for small earthquakes and the scaling of local to moment magnitude, *Geophysical Journal International*, 183, no. 1, 407–420, doi: [10.1111/j.1365-246X.2010.04743.x](https://doi.org/10.1111/j.1365-246X.2010.04743.x)
- Edwards B, Kraft T, Cauzzi C, et al (2015). Seismic monitoring and analysis of deep geothermal projects in St Gallen and Basel, Switzerland. *Geophys J Int* 201:1022–1039. doi: 10.1093/gji/ggv059
- EFEHR. (2022). Earthquake Hazard & Risk across Europe. EFEHR. <http://www.efehr.org/start/>
- Erdik, M., Sesetyan, K., Demircioglu, M. et al. (2010). Rapid earthquake hazard and loss assessment for Euro-Mediterranean region. *Acta Geophys.* 58, 855–892, <https://doi.org/10.2478/s11600-010-0027-4>
- Faenza L, Michelini A (2010). Regression analysis of MCS intensity and ground motion parameters in Italy and its application in ShakeMap. *Geophys. J. Int.* 180:1138–1152
- Faenza L, Michelini A (2011). Regression analysis of MCS intensity and ground motion spectral accelerations (SAs) in Italy. *Geophys. J. Int.* 186:1415–1430
- Fäh D, Fritsche S, Poggi V, et al., (2009). Determination of site information for seismic stations in Switzerland, Swiss Seismological Service technical report: SED/PRP/R/004/20090831
- Fäh, D., Giardini, D., Kästli, P., et al. (2011). ECOS-09 earthquake catalogue of Switzerland release 2011 report and database. Public catalogue, 17. 4. 2011, Swiss Seismological Service ETH Zurich, Report SED/RISK/R/001/20110417
- Fäh D. et al., 2012. Coupled seismogenic geohazards in Alpine regions. *Bollettino di Geofisica Teorica ed Applicata* 53(4), 485-508
- Fallou, L., Marti, M., Dallo, I., & Corradini, M. (2022). How to fight earthquake misinformation: A communication guide. *Seismological Research Letters*. <https://doi.org/10.1785/0220220086>
- Flores-Saviaga, C., & Savage, S. (2020). Fighting disaster misinformation in Latin America: The #19S Mexican earthquake case study. *Personal and Ubiquitous Computing*. <https://doi.org/10.1007/s00779-020-01411-5>
- Field, E. H., Jordan, T. H., Page, M. T., Milner, K. R., Shaw, B. E., Dawson, T. E., ... & Thatcher, W. R. (2017). A synoptic view of the third Uniform California Earthquake Rupture Forecast (UCERF3). *Seismological Research Letters*, 88(5), 1259-1267.
- Federal Office for Civil Protection (FOCP) (2020): National risk analysis report, Disasters and Emergencies in Switzerland 2020. FOCP, Bern. [babs.admin.ch/en/aufgabenbabs/gefaehdrisiken/natgefaehrdanalyse.html](https://www.babs.admin.ch/en/aufgabenbabs/gefaehdrisiken/natgefaehrdanalyse.html)
- Fritsche S, & Fäh D. (2009). The 1946 magnitude 6.1 earthquake in the Valais: site-effects as contributor to the damage. *Swiss Journal of Geosciences* 102, 423
- Fritsche, S. al. (2012). Historical intensity VIII earthquakes along the Rhone valley (Valais, Switzerland): primary and secondary effects. *Swiss J Geosci* 105, 1–18.
- Giardini, D., Wiemer, S., Fäh, D., and Deichmann, N., 2004. *Seismic Hazard Assessment of Switzerland, 2004*. GFZ Helmholtz Centre Potsdam German Research Centre for Geosciences and gempa GmbH (2008). The SeisComp seismological software package. GFZ Data Services. doi:10.5880/GFZ.2.4.2020.003
- Glueer F., et al. (2021). Coseismic Stability Assessment of a Damaged Underground Ammunition Storage Chamber Through Ambient Vibration Recordings and Numerical Modelling. *Front. Earth Sci.* 9:773155
- Gómez-García, C., Brenguier, F., Boué, P., Shapiro, N. M., Droznin, D. V., Droznina, S. Y., et al. (2018). Retrieving robust noise-based seismic velocity changes from sparse data sets: Synthetic tests and application to Klyuchevskoy volcanic group (Kamchatka). *Geophysical Journal International*, 214(2), 1218–1236.
- Gulia, L., and S. Wiemer (2019). Real-time discrimination of earthquake foreshocks and aftershocks, *Nature* 574, 193–200, doi: 10.1038/s41586-019-1606-4.
- Häusler M. et al., 2021. Monitoring the Preonzo Rock Slope Instability Using Resonance Mode Analysis. *JGR Earth Surface*, 126(4), e2020JF005709
- Häusler M. et al., 2022. Monitoring the changing seismic site response of a fast-moving rockslide (Brien/Brinzauls, Switzerland). *Geophysical Journal International*, 229(1), 299–310
- Hailemichael S, Amoroso S, Gaudiosi I (2020). Guest editorial: seismic microzonation of Central Italy following the 2016–2017 seismic sequence. *Bulletin of Earthquake Engineering* 18:5415–5422
- Hanka, W. et al. (2010). Real-time earthquake monitoring for tsunami warning in the Indian Ocean and beyond. *Natural Hazards and Earth System Science* 10, 2611–2622.

- Hardebeck, J. L., and P. M. Shearer (2002). A new method for determining first-motion focal mechanisms, *Bull. Seismol. Soc. Am.* 92, no. 6, 2264–2276, doi: 10.1785/0120010200.
- Heimann, S., M. Isken, D. Kühn, H. Sudhaus, A. Steinberg, H. Vasyura-Bathke, S. Daout, S. Cesca, and T. Dahm (2018). Grond - A probabilistic earthquake source inversion framework., GFZ Data Services, doi: 10.5880/GFZ.2.1.2018.003.
- Helmholtz Centre Potsdam GFZ German Research Centre for Geosciences and gempa GmbH (2008). *The SeisComP seismological software package*. GFZ Data Services. doi:10.5880/GFZ.2.4.2020.003.
- Hengl T, Heuvelink GBM, Rossiter DG (2007). About regression-kriging: From equations to case studies. *Computers & Geosciences* 33(10):1301-1315
- Hilbe, M., & Anselmetti, F. S., 2014. Signatures of slope failures and river-delta collapses in a perialpine lake (Lake Lucerne, Switzerland). *Sedimentology* 61, 1883–1907.
- Hobbs, T. E., & Rollins, C. (2019). Earthquake early warning system challenged by the largest SoCal shock in 20 years. *Temblor*. <http://doi.org/10.32858/temblor.035>
- Hobiger M, Bergamo P, Imperatori W, Panzera F, Lontsi AM, Perron V, Michel C, Burjáněk J., Fäh D (2021). Site Characterization of Swiss Strong Motion Stations: The Benefit of Advanced Processing Algorithms. *Bulletin of the Seismological Society of America* 2021 111 (4):1713–1739
- Husen, S., E. Kissling, N. Deichmann, S. Wiemer, D. Giardini, and M. Baer (2003). Probabilistic earthquake location in complex three-dimensional velocity models: Application to Switzerland, *Journal of Geophysical Research-Solid Earth*, 108, no. B2.
- Janusz P. et al. (2022a). Calibration of soil dilatancy parameters using CPT data – the case of Lucerne in central Switzerland. 3rd European Conference on Earthquake Engineering & Seismology Bucharest, Romania, 2022, extended abstract 4747- 4756.
- Janusz P. et al. (2022b). A case study on non-linear soil response in urban areas. URBASIS-EU, Work Package 3, deliverable D3.2, https://urbasis-eu.osug.fr/IMG/pdf/wp3-d3.2_-_a_case_study_on_non-linear_soil_response_in_urban_areas.pdf
- Janusz, P. et al. (2022c). Preliminary results of estimating the non-linear site response in the Lucerne area. Abstract Volume 20th Swiss Geoscience Meeting 2022, Lausanne, Switzerland, 250-250
- Janusz P, Perron V, Knellwolf C, Fäh D (2022d) Combining Earthquake Ground Motion and Ambient Vibration Recordings to Evaluate a Local High-Resolution Amplification Model—Insight from the Lucerne Area, Switzerland. *Front. Earth Sci.* 10:885724
- Jozinović, D., F. Massin, M. Böse, and J. Clinton (2023). Combining earthquake early warning solutions from different algorithms: application to Switzerland, SSA abstract 2023.
- Juretzek, C., & Hadziioannou, C. (2016). Where do ocean microseisms come from? A study of Love to Rayleigh wave ratios. *Journal of Geophysical Research: Solid Earth*, 121, 6741–6756. <https://doi.org/10.1002/2016JB013017>
- Kastrup, U., M. L. Zoback, N. Deichmann, K. F. Evans, D. Giardini, and A. J. Michael, 2004, Stress field variations in the Swiss Alps and the northern Alpine foreland derived from inversion of fault plane solutions, *J. Geophys. Res.*, 109, no. B1, doi: 10.1029/2003JB002550.
- Kremer K., et al., 2012. Giant Lake Geneva tsunami in AD 563. *Nature Geoscience* 5(11):756-757
- Kremer K., et al., 2017. Lake-sediment based paleoseismology: limitations and perspectives from the Swiss Alps. *Quat Sci Rev* 168, 1 – 18
- Kremer K., et al., 2020. A database of potential paleoseismic evidence in Switzerland. *J Seismol* 24, 247–262.
- Kremer K., et al., 2022. Traces of a prehistoric and potentially tsunamigenic mass movement in the sediments of Lake Thun (Switzerland). *Swiss J Geosci* 115, 13.
- Kleinbrod U. et al., 2017a. A comparative study on seismic response of two unstable rock slopes within same tectonic setting but different activity level. *Geophysical Journal International*, 211(3), 1428–1448
- Kleinbrod U. et al., 2017b. On the seismic response of instable rock slopes based on ambient vibration recordings. *Earth Planets Space* 69, 126
- Kleinbrod U. et al., 2018. Ambient vibration classification of unstable rock slopes: A systematic approach. *Engineering Geology*, 249, 198-217.
- Kwiatak, G., P. Martínez-Garzón, and M. Bohnhoff (2016). HybridMT: A MATLAB/Shell Environment Package for Seismic Moment Tensor Inversion and Refinement, *Seismol. Res. Lett.* 87, no. 4, 964–976, doi: 10.1785/0220150251.
- Lang, D. J., Wiek, A., Bergmann, M., Stauffacher, M., Martens, P., Moll, P., Swilling, M., & Thomas, C. J. (2012). Transdisciplinary research in sustainability science: Practice, principles, and challenges. *Sustainability Science*, 7(1), 25–43. <https://doi.org/10.1007/s11625-011-0149-x>
- Lanza, F., T. Diehl, N. Deichmann, T. Kraft, C. Nussbaum, S. Schefer, and S. Wiemer (2022). The Saint-Ursanne earthquakes of 2000 revisited: evidence for active shallow thrust-faulting in the Jura fold-and-thrust belt, *Swiss J Geosci*, 115, no. 1, 2, doi: 10.1186/s00015-021-00400-x.
- Lee, T., T. Diehl, E. Kissling, and S. Wiemer (2023). New insights into the Rhône–Simplon fault system (Swiss Alps) from a consistent earthquake catalogue covering 35 yr, *Geophysical Journal International*, 232, no. 3, 1568–1589, doi: 10.1093/gji/ggac407.
- Lee, T. (2023). The transition between Western and Central Alps: New seismotectonic insights from high-resolution earthquake catalogs and tomography, Ph.D. Thesis, ETH Zurich.
- Lobbis, O., and R. Weaver (2003), Coda-wave interferometry in finite solids: Recovery of P-to-S conversion rates in an elastodynamic billiard, *Phys. Rev. Lett.*, 90, 254302.

- Lontsi A.M. et al., 2022. A Robust Workflow for Acquiring and Preprocessing Ambient Vibration Data from Small Aperture Ocean Bottom Seismometer Arrays to Extract Scholte and Love Waves Phase-Velocity Dispersion Curves. *Pure and Applied Geophysics* 179, 105–123
- Lu, Y., Pedersen, H. A., Stehly, L., & AlpArray Working Group. (2022). Mapping the seismic noise field in Europe: spatio-temporal variations in wavefield composition and noise source contributions. *Geophysical Journal International*, 228(1), 171-192.
- Luoni, G., Dallo, I., Marti, M., Freeman, A. L. J., & Dryhurst, S. (2021). Current communication pathways for seismic information in Italy, Switzerland and Iceland (Society: Data Gathering and Information Sharing with the Public and Policy-Makers) [Deliverable]. European Horizon-2020 project RISE. http://static.seismo.ethz.ch/rise/deliverables/Deliverable_5.2.pdf
- Marschall, I., N. Deichmann, and F. Marone, 2013, Earthquake focal mechanisms and stress orientations in the eastern Swiss Alps, *Swiss Journal of Geosciences*, 106, no. 1, 79–90.
- Martakis, P., Reuland, Y., Stavridis, A., & Chatzi, E. (2023). Fusing damage-sensitive features and domain adaptation towards robust damage classification in real buildings. *Soil Dynamics and Earthquake Engineering*, 166, 107739.
- Martakis, P., Movsessian, A., Reuland, Y., Pai, S. G., Quqa, S., Garcia Cava, D., Tcherniak, D., & Chatzi, E. (2022a). A semi-supervised interpretable machine learning framework for sensor fault detection. *Smart Struct. Syst. Int. J.*, 29, 251-266.
- Martakis, P., Reuland, Y., Imesch, M., & Chatzi, E. (2022b). Reducing uncertainty in seismic assessment of multiple masonry buildings based on monitored demolitions. *Bulletin of Earthquake Engineering*, 20(9), 4441-4482.
- Martakis, P., Reuland, Y., & Chatzi, E. (2020). Amplitude-dependent model updating of masonry buildings undergoing demolition.
- Marti, M., Dallo, I., Roth, P., Papadopoulos, A. N., & Zaugg, S. (2022). Illustrating the impact of earthquakes: Evidence-based and user-centered recommendations on how to design earthquake scenarios and rapid impact assessments. Submitted to *International Journal of Disaster Risk Reduction*.
- Marti, M., Stauffacher, M., & Wiemer, S. (2019). Difficulties in explaining complex issues with maps. Evaluating seismic hazard communication – the Swiss case. *Natural Hazards and Earth System Sciences*, 19(12), Article 12.
- Marti, M., Stauffacher, M., & Wiemer, S. (2020). Anecdotal evidence is an insufficient basis for designing earthquake preparedness campaigns. *Seismological Research Letters*, 91(4), Article 4. <https://doi.org/10.1785/0220200010>
- Marzocchi, W., Lombardi, A. M., & Casarotti, E. (2014). The establishment of an operational earthquake forecasting system in Italy. *Seismological Research Letters*, 85(5), 961-969.
- Massin, F., J. Clinton, and M. Böse (2021). Status of Earthquake Early Warning in Switzerland, *Front. Earth Sci.* 9, doi:10.3389/feart.2021.707654.
- Massin, F., Clinton, J., Racine, R., Böse, M., Rossi, Y., Marroquin, G., et al. (2020). "The Future strong Motion National Seismic Networks in Central America Designed for Earthquake Early Warning," in EGU General Assembly Conference Abstracts, Vienna, Austria, 19437, doi:10.1785/0220200043.
- Melles, G., Howard, Z., & Thompson-Whiteside, S. (2012). Teaching design thinking: Expanding horizons in design education. *Procedia - Social and Behavioral Sciences*, 31, 162–166. <https://doi.org/10.1016/j.sbspro.2011.12.035>
- Mero, A. (2019). In quake-rattled Albania, journalists detained on fake news charges after falsely warning of aftershocks. *Voice of America (VOC)*. https://www.voanews.com/a/europe_quake-rattled-albania-journalists-detained-fake-news-charges-after-falsely-warning/6176290.html
- Mesimeri, M., D. Armbruster, P. Kaestli, L. Scarabello, T. Diehl, J. Clinton, and S. Wiemer (2023). SCDetect: Real-time computationally efficient waveform cross-correlation based earthquake detection. To be submitted to *SRL*.
- Michel C, Edwards B, Poggi V, Burjánek J, Fäh D (2014). Assessment of Site Effects in Alpine Regions through Systematic Site Characterization of Seismic Stations. *Bulletin of the Seismological Society of America* 104(6):2809–2826
- Michel C, Fäh D, Edwards B, Cauzzi CV (2017). Site amplification at the city scale in Basel (Switzerland) from geophysical site characterization and spectral modelling of recorded earthquakes. *Physics and Chemistry of the Earth* 98:27-40.
- Minson, S. E., Wu, S., Beck, J. L., and Heaton, T. H. (2017). Combining Multiple Earthquake Models in Real Time for Earthquake Early Warning, *Bull. Seismol. Soc. Am.* 107(4), 1868–1882, doi:10.1785/0120160331.
- Mitchell-Wallace, K., Jones, M., Hillier, J., and Foote, M., 2017. *Natural catastrophe risk management and modelling. Natural catastrophe risk management and modelling: A practitioner's Guide (1st ed.)*. Hoboken, NJ: John Wiley & Sons, Ltd. DOI: 10.1002/9781118906057.
- Mizrahi, L., S. Nandan, and S. Wiemer (2021). Embracing Data Incompleteness for Better Earthquake Forecasting, *J. Geophys. Res. Solid Earth*, 1–26, doi: 10.1029/2021JB022379.
- Mizrahi, L., Schmid, N., Han, M. (2023). Imizrahi/etas: ETAS with fit visualization (3.2). Zenodo. <https://doi.org/10.5281/zenodo.7584575>
- Mizrahi, L., Nandan, S., Wiemer, S. Developing and Testing ETAS-Based Earthquake Forecasting Models for Switzerland. In preparation.
- Moroney, L. *Firestore Cloud Messaging*. in *The Definitive Guide to Firebase* 163–188 (Apress, 2017). doi:10.1007/978-1-4842-2943-9_9.
- Nandan, S., Kamer, Y., Ouillon, G., Hiemer, S., & Sornette, D. (2021). Global models for short-term earthquake forecasting and predictive skill assessment. *The European Physical Journal Special Topics*, 230(1), 425-449.
- Nievas, C., et al. (2023). RISE deliverable 6.1: Integration of RISE Innovations in the Fields of OELF, RLA and SHM. (in preparation)

- Obermann, A., Lupi, M., Mordret, A., Jakobsdóttir, S.S., Miller, S.A., 2016. 3D-ambient noise Rayleigh wave tomography of Snæfellsjökull volcano, Iceland. *J. Vol. Geotherm. Res.* 317, 42–52. <https://doi.org/10.1016/j.jvolgeores.2016.02.013>.
- Ogata, Y. (1988). Statistical models for earthquake occurrences and residual analysis for point processes. *Journal of the American Statistical Association*, 83(401), 9-27.
- Ogata, Y., Katsura, K., Falcone, G., Nanjo, K., & Zhuang, J. (2013). Comprehensive and topical evaluations of earthquake forecasts in terms of number, time, space, and magnitude. *Bulletin of the Seismological Society of America*, 103(3), 1692-1708.
- Pagani, M., Monelli, D., Weatherill, G., Danciu, L., Crowley, H., Silva, V., Henshaw, P., et al., 2014. OpenQuake Engine: An Open Hazard (and Risk) Software for the Global Earthquake Model. *Seismological Research Letters*, 85(3), 692–702. DOI: 10.1785/0220130087
- Panzerä F, Bergamo P, Föh D, 2021. Canonical Correlation Analysis Based on Site-Response Proxies to Predict Site-Specific Amplification Functions in Switzerland. *Bulletin of the Seismological Society of America*, 111 (4): 1905–1920
- Panzerä F, Alber J, Imperatori W, Bergamo P, Föh D, 2022. Reconstructing a 3D model from geophysical data for local amplification modelling: The study case of the upper Rhone valley, Switzerland. *Soil Dynamics and Earthquake Engineering*, 155, 107163
- Papadopoulos, A.N, M. Böse, L. Danciu, J. Clinton, and S. Wiemer (2023). Effectiveness of Earthquake Early Warning in Mitigating Seismic Risk, *Earthquake Spectra*, accepted.
- Peary, B. D. M., Shaw, R., & Takeuchi, Y. (2012). Utilization of Social Media in the East Japan Earthquake and Tsunami and its Effectiveness. *Journal of Natural Disaster Science*, 34(1), Article 1. <https://doi.org/10.2328/jnds.34.3>
- Perron V, Bergamo P, Föh D. (2022). Site Amplification at High Spatial Resolution from Combined Ambient Noise and Earthquake Recordings in Sion, Switzerland. *Seismological Research Letters*, 93 (4): 2281–2298
- Poggi V, Edwards B, Föh D (2011). Derivation of a reference shear-wave velocity model from empirical site amplification. *Bull Seismol Soc Am* 101:258–274. <https://doi.org/10.1785/0120100060>
- Poggi V, Burjánek J, Michel C, Föh D (2017). Seismic siteresponse characterization of high-velocity sites using advanced geophysical techniques: application to the NAGRANet. *Geophys J Int* 210:645–659. <https://doi.org/10.1093/gji/ggx192>
- Porras, J., F. Massin, M. Arroyo-Solórzano, I. Arroyo, L. Linkimer, M. Böse and J. Clinton (2021). Preliminary Results of an Earthquake Early Warning System in Costa Rica. *Front. Earth Sci.* 9:700843. doi: 10.3389/feart.2021.700843.
- Racine R, Cauzzi C, Clinton J, et al. (2020). Updated determination of earthquake magnitudes at the Swiss Seismological Service. EGU2020-8273.
- Reuland, Y., Bodenmann, L., Blagojevic, N., & Stojadinovic, B. (2022). Deliverable 4.4 Development of RRE forecasting services in OpenQuake.
- Reuland, Y., Martakis, P., & Chatzi, E. (2023). A comparative study of damage-sensitive features for rapid data-driven seismic structural-health monitoring. *Applied Sciences*. *Under Review*.
- Reuland, Y., Martakis, P., & Chatzi, E. (2022). RISE deliverable 4.5: The use of structural health monitoring for rapid loss assessment
- Reuland, Y., Martakis, P., & Chatzi, E. (2021). Damage-sensitive features for rapid damage assessment in a seismic context. In *Proc. of the International Conference on Structural Health Monitoring of Intelligent Infrastructure* (pp. 613-619). International Society for Structural Health Monitoring of Intelligent Infrastructure (ISHMII).
- Rhoades, D. A., Liukis, M., Christophersen, A., & Gerstenberger, M. C. (2016). Retrospective tests of hybrid operational earthquake forecasting models for Canterbury. *Geophysical Journal International*, 204(1), 440-456.
- Roten D. et al. (2009). Estimation of non-linear site response in a deep Alpine valley. *Geophysical Journal International*, 178(3), 1597–1613.
- Roten D. (2014). Documentation of tools for analysis of nonlinear soil behavior.
- Roten D. et al. (2014). Quantification of Cyclic Mobility Parameters in Liquefiable Soils from Inversion of Vertical Array Records. *Bulletin of the Seismological Society of America*, 104, 3115–3138.
- Savran, W. H., Werner, M. J., Marzocchi, W., Rhoades, D. A., Jackson, D. D., Milner, K., ... & Michael, A. (2020). Pseudoprospective evaluation of UCERF3-ETAS forecasts during the 2019 Ridgecrest sequence. *Bulletin of the Seismological Society of America*, 110(4), 1799-1817.
- Sánchez-Pastor, P., Obermann, A., Schimmel, M. (2018). Detecting and locating precursory signals during the 2011 El Hierro, Canary Islands, submarine eruption. *Geophys. Res. Lett.* 45 (19), 10–288. <https://doi.org/10.1029/2018GL079550>.
- Sens-Schönfelder, C., and U. Wegler (2006). Passive image interferometry and seasonal variations of seismic velocities at Merapi Volcano, Indonesia. *Geophys. Res. Lett.*, 33, L21302, doi:10.1029/2006GL027797.
- Silva, V., Amo-Oduro, D., Calderon, A., Costa, C., Dabbeek, J., Despotaki, V., Martins, L., et al. (2020). Development of a global seismic risk model. *Earthquake Spectra*, (February), 875529301989995. DOI: 10.1177/8755293019899953.
- Shi, P., F. Grigoli, F. Lanza, G. C. Beroza, L. Scarabello, and S. Wiemer (2022). MALMI: An Automated Earthquake Detection and Location Workflow Based on Machine Learning and Waveform Migration. *Seismological Research Letters* 93 (5): 2467–2483. doi: <https://doi.org/10.1785/0220220071>.
- Shynkarenko, A., et al. (2021). Investigating the subsurface in a shallow water environment using array and single-station ambient vibration techniques. *Geophysical Journal International* 227(3):1857–1878
- Shynkarenko, A., et al. (2022). Geotechnical characterization and stability analysis of subaqueous slopes in Lake Lucerne (Switzerland). *Nat Hazards* 113, 475–505

- Shynkarenko, A., et al. (2023). On the seismic response and earthquake-triggered failures of subaqueous slopes in Swiss lakes. *Geophysical Journal International*, under review.
- Shynkarenko A. (2023). Characterization of structure and stability of subaqueous lake slopes using seismological and geotechnical data. PhD thesis, ETH Zurich.
- Sokos, E. N., and J. Zahradnik (2013). Evaluating Centroid-Moment-Tensor Uncertainty in the New Version of ISOLA Software, *Seismol. Res. Lett.* 84, no. 4, 656–665, doi: 10.1785/0220130002.
- Stehly, L., Fry, B., Campillo, M., Shapiro, N.M., Guilbert, J., Boschi, L., Giardini, D. (2009). Tomography of the Alpine region from observations of seismic ambient noise. *Geophys. J. Int.* 178 (1), 338–350. <https://doi.org/10.1111/j.1365-246X.2009.04132.x>.
- Strader, A., Schneider, M., & Schorlemmer, D. (2017). Prospective and retrospective evaluation of five-year earthquake forecast models for California. *Geophysical Journal International*, 211(1), 239–251.
- Strupler M. et al. (2018). Subaqueous landslide-triggered tsunami hazard for Lake Zurich, Switzerland. *Swiss Journal of Geosciences* 111, 353–371
- Strupler M. et al. (2020). A workflow for the rapid assessment of the landslide-tsunami hazard in peri-alpine lakes. *Geological Society London Special Publications* 500(1).
- Stutzmann, E., Schimmel, M., Patau, G., & Maggi, A. (2009). Global climate imprint on seismic noise. *Geochemistry, Geophysics, Geosystems*, 10, Q11004. <https://doi.org/10.1029/2009GC002619>.
- Strollo, A., M. Cambiz, J. Clinton et al. (2021) EIDA: The European Integrated Data Archive and Service Infrastructure within ORFEUS, *Seismological Research Letters* 92(3). DOI:10.1785/0220200413
- Swiss Seismological Service (SED) At ETH Zurich (1983). National Seismic Networks of Switzerland. Other/Seismic Network. Zurich: ETH Zürich. doi:10.12686/sed/networks/ch
- Swiss Seismological Service (SED) at ETH Zurich (2015). The Site Characterization Database for Seismic Stations in Switzerland. Zurich: Federal Institute of Technology. doi: 10.12686/sed-stationcharacterizationdb (<http://stations.seismo.ethz.ch>).
- Swisstopo, Swiss Federal Office of Topography (2019). Felsoberflächenmodell (TopFels25). <https://www.swisstopo.admin.ch/en/geodata/geology/models.html> accessed 04.06.2019
- Vackář, J., J. Burjánek, F. Gallovič, J. Zahradník, and J. Clinton, 2017, Bayesian ISOLA: new tool for automated centroid moment tensor inversion, *Geophysical Journal International*, 210, no. 2, 693–705, doi: 10.1093/gji/ggx158.
- Valenzuela Rodríguez, N. (2021). Die aktuelle Erdbebensituation der Schweiz visualisieren—Eine Analyse der Erdbekanntkarte der MeteoSchweiz-App hinsichtlich ihrer Verständlichkeit und ihres Verbesserungspotenzials [Master Thesis, Zurich University of Applied Sciences (ZHAW)]. <https://www.polybox.ethz.ch/index.php/s/vaBmjfUr0AgaVtS>
- van der Elst, N. J., Hardebeck, J. L., Michael, A. J., McBride, S. K., & Vanacore, E. (2022). Prospective and retrospective evaluation of the US Geological Survey Public aftershock forecast for the 2019–2021 Southwest Puerto Rico Earthquake and aftershocks. *Seismological Society of America*, 93(2A), 620–640.
- Vilanova SP, Narciso J, Carvalho JP, Lopes I, Quinta Ferreira M, Pinto CC, Moura R, Borges J, Nemser ES (2018). Developing a Geologically Based VS30 Site Condition Model for Portugal: Methodology and Assessment of the Performance of Proxies. *Bulletin of the Seismological Society of America* 108(1):322–337.
- Wald, D.J., Jaiswal, K.S., Marano, K.D., Bausch, D.B., and Hearne, M.G. (2010). PAGER—Rapid assessment of an earthquake's impact: U.S. Geological Survey Fact Sheet 2010–3036, 4 p. Revised November, 2011.
- Waldhauser, F., and W. L. Ellsworth (2000). A double-difference earthquake location algorithm: method and application to the northern Hayward fault, California, *Bulletin of the Seismological Society of America*, 90, no. 6, 1353–1368.
- Waldhauser, F. (2009). Near-Real-Time Double-Difference Event Location Using Long-Term Seismic Archives, with Application to Northern California, *Bulletin of the Seismological Society of America*, 99, no. 5, 2736–2748.
- Weatherill, G., Crowley, H., Roullé, A. et al. (2022). Modelling site response at regional scale for the 2020 European Seismic Risk Model (ESRM20). *Bull Earthquake Eng* (2022). <https://doi.org/10.1007/s10518-022-01526-5>
- Weaver, R.L., Lobkis, O.I. (2001a). Ultrasonics without a source: Thermal fluctuation correlation at MHz frequencies. *Phys. Rev. Lett.* 87, 134301 <https://doi.org/10.1103/PhysRevLett.87.134301>.
- Weber S. et al. (2021). Spectral amplification of ground motion linked to resonance of large-scale mountain landforms. *Earth and Planetary Sciences Letters* 578(8):117295
- Wiemer, S. L. Danciu, B. Edwards, M. Marti, D. Fäh, S. Hiemer, J. Wössner, C. Cauzzi, P. Kästli, and K. Kremer (2016). Seismic Hazard Model 2015 for Switzerland (SULhaz2015), report, Swiss Seismological Service (SED) at ETH Zurich. Retrieved from <http://www.seismo.ethz.ch/en/knowledge/seismic-hazard/maps>, doi:10.12686/a2.
- Woessner, J., Hainzl, S., Marzocchi, W., Werner, M. J., Lombardi, A. M., Catali, F., ... & Wiemer, S. (2011). A retrospective comparative forecast test on the 1992 Landers sequence. *Journal of Geophysical Research: Solid Earth*, 116(B5).
- Worden, C.B., E. M. Thompson, M. Hearne, and D.J. Wald (2020). ShakeMap Manual Online: technical manual, user's guide, and software guide, U. S. Geological Survey. <http://cbworden.github.io/shakemap/>. DOI: <https://doi.org/10.5066/F7D21VPQ>.